

Developmental and biophysical determinants of grass leaf size worldwide

<https://doi.org/10.1038/s41586-021-03370-0>

Received: 11 October 2019

Accepted: 18 February 2021

Published online: 24 March 2021

 Check for updates

Alec S. Baird¹✉, Samuel H. Taylor^{2,3}, Jessica Pasquet-Kok¹, Christine Vuong¹, Yu Zhang¹, Teera Watcharamongkol^{3,4}, Christine Scoffoni^{1,5}, Erika J. Edwards⁶, Pascal-Antoine Christin³, Colin P. Osborne³ & Lawren Sack¹✉

One of the most notable ecological trends—described more than 2,300 years ago by Theophrastus—is the association of small leaves with dry and cold climates, which has recently been recognized for eudicotyledonous plants at a global scale^{1–3}. For eudicotyledons, this pattern has been attributed to the fact that small leaves have a thinner boundary layer that helps to avoid extreme leaf temperatures⁴ and their leaf development results in vein traits that improve water transport under cold or dry climates^{5,6}. However, the global distribution of leaf size and its adaptive basis have not been tested in the grasses, which represent a diverse lineage that is distinct in leaf morphology and that contributes 33% of terrestrial primary productivity (including the bulk of crop production)⁷. Here we demonstrate that grasses have shorter and narrower leaves under colder and drier climates worldwide. We show that small grass leaves have thermal advantages and vein development that contrast with those of eudicotyledons, but that also explain the abundance of small leaves in cold and dry climates. The worldwide distribution of leaf size in grasses exemplifies how biophysical and developmental processes result in convergence across major lineages in adaptation to climate globally, and highlights the importance of leaf size and venation architecture for grass performance in past, present and future ecosystems.

The grasses (Poaceae), which originated at least 55 million years ago⁸, comprise about 11,500 species in 750 genera⁹ and dominate up to 43% of the land surface of the Earth⁷ (Fig. 1). Small leaves have previously been linked with arid climates in specific grass lineages and communities (see Supplementary Table 1 for a summary of the relevant publications). A worldwide climatic association could be an important influence on the distributions of grass species and their tolerance of climate change, as well as on crop breeding. We tested relationships of leaf size with climate across 1,752 grass species from 373 genera in a global database, and for 27 diverse and globally distributed species in a common garden (Extended Data Fig. 1, Supplementary Tables 2, 3).

We also tested for an adaptive basis for the association of grass leaf size with climate (Fig. 1). Because smaller leaves couple more tightly with air temperature (owing to their thinner boundary layer), small-leaved eudicotyledons avoid damage from night-time chilling and daytime overheating⁴; smaller leaves may also achieve a higher photosynthetic rate and water-use efficiency, and compensate for shorter growing periods^{4,10–12}. We evaluated these potential advantages for small-leaved grasses using energy balance modelling.

Smaller leaves may also develop vein traits that confer stress tolerance⁵. In typical eudicotyledons the large ('major') veins are patterned before the bulk of leaf expansion⁵; leaves that expand less have narrower major veins and xylem conduits, and major veins that are more closely spaced, which results in a higher vein length per leaf area (VLA)

of their major veins^{5,6}. Across eudicotyledons, major vein traits scale allometrically with mature leaf size: trait = $a \times \text{leaf area}^b$ (in which a is a scaling coefficient and b is the scaling exponent)¹³. The major vein traits in small leaves of eudicotyledons can provide greater water transport and lower vulnerability to freezing and dehydration⁶ (Fig. 1a, Supplementary Table 4). However, grass leaves are highly distinct from those of eudicotyledons, far smaller on average, and characterized by parallel longitudinal veins connected by transverse veins¹⁴. To determine vein scaling and its adaptive consequences for small leaves in grasses, we synthesized a model of leaf development for C₃ and C₄ grasses (Table 1, Box 1).

Developmental scaling of grass venation

Our synthetic model of leaf development in grasses (Box 1) is conserved across grass species, and therefore scaling predictions can be derived for species that vary in leaf size (Supplementary Tables 5, 6). Some of these scaling relationships arise intrinsically from the sequence of development: for example, major VLA is lower in wider leaves, as their major veins are spaced further apart. In the model, VLA for first-order veins declines geometrically as the inverse of leaf width, whereas the VLA for second-order veins declines less steeply than geometrically (because the formation of more second-order veins partially counteracts their greater spacing). Other scaling trends are not intrinsic,

¹Department of Ecology and Evolutionary Biology, University of California Los Angeles, Los Angeles, CA, USA. ²Lancaster Environment Centre, University of Lancaster, Lancaster, UK.

³Department of Animal and Plant Sciences, University of Sheffield, Sheffield, UK. ⁴Faculty of Science and Technology, Kanchanaburi Rajabhat University, Kanchanaburi, Thailand. ⁵Department of Biological Sciences, California State University Los Angeles, Los Angeles, CA, USA. ⁶Department of Ecology and Evolutionary Biology, Yale University, New Haven, CT, USA. ✉e-mail: alecsbaird@gmail.com; lawrensack@ucla.edu

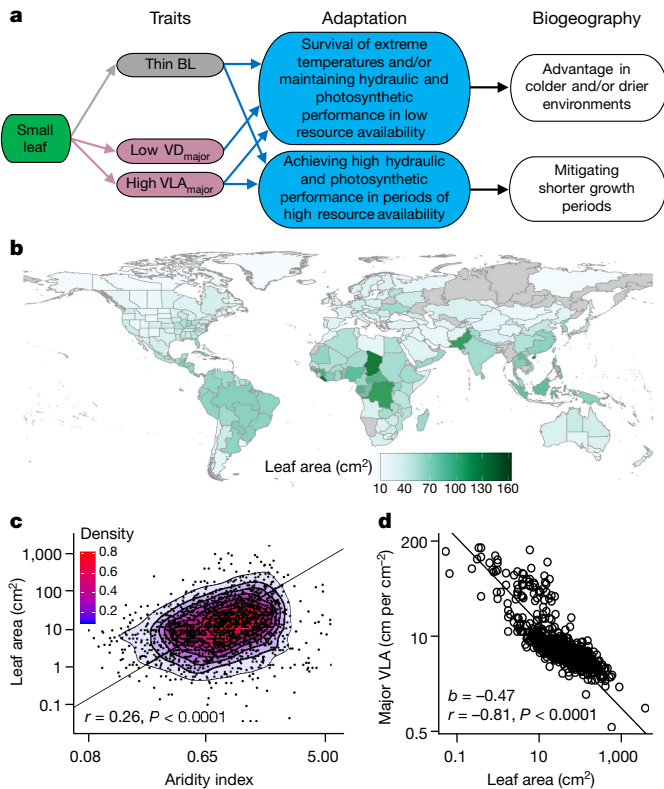


Fig. 1 | Relationship of grass leaf size, traits and climatic distribution of species worldwide. **a**, Links between small leaf size and traits, adaptation to cold and dry climates, and biogeography, as established for eudicotyledons (Supplementary Table 4) and hypothesized for grasses. Small leaves have thin boundary layers (BL), develop lower major vein diameters (VD_{major}) and have higher major VLA (VLA_{major}), which provide advantages in cold or dry climates (Supplementary Table 4). Large leaves would be disadvantaged in such climates (relative to warm and moist climates). **b**, Grass leaf area averaged per country in the global database (across-species mean of leaf area for 21 to 547 species per country; grey denotes that <20 species are represented). **c**, Grass leaf area in relation to the aridity index (a low index reflects a drier climate). Each point represents a species ($n=912$ C₃ and 840 C₄ species). Contour lines and colours represent the 2D kernel density of points. **d**, The association of VLA_{major} with leaf area across grass species ($n=600$ species). Statistics represent the fits for $\log(y) = \log(a) + b \log(x)$ from ordinary least squares in **c**, **d**. $P=2.3 \times 10^{-27}$ (**c**), 1.6×10^{-139} (**d**) (both two-tailed).

but are instead ‘enabled’ by the developmental program¹⁵. The diameters of first- and second-order veins are expected to scale positively with leaf length and area, because a greater rate or duration of leaf length expansion enables a greater growth of vein diameters. Similarly, a positive scaling of the diameters of first- and second-order vein xylem conduits with vein diameter is enabled by the greater vein expansion in larger leaves.

Minor veins differ from major veins in their predicted scaling with leaf size across species. As minor veins are initiated at the tip of the developing leaf, greater length expansion provides more space and time for initiating additional minor veins. Minor VLA therefore scales positively with final leaf length. However, as minor veins are initiated later during leaf-width expansion and their diameter growth and spacing is more limited than that of major veins, their vein traits are independent of final width. The positive scaling of minor VLA with leaf length, and its decoupling from leaf width, would result in weak scaling of minor VLA with leaf area. Total VLA (that is, summing major and minor veins) is decoupled from leaf area, owing to the negative scaling of major VLA with leaf width and the positive scaling of minor VLA with leaf length. Additional scaling predictions arise from the relationships of

vein diameters and lengths with leaf size (Supplementary Table 6). As with the diameters of major veins, the major vein surface area, vein projected area and vein volume per unit leaf area (VSA, VPA and VVA, respectively) scale positively with leaf length and—similar to major VLA—negatively with leaf width. These counteracting trends lead to predictions that VSA, VPA and VVA are decoupled from leaf area.

Our developmental model predicts that grass species with smaller leaf dimensions will develop vein traits that confer stress tolerance; these traits include narrower major veins and higher major VLA, VSA, VPA and VVA, which contribute to water transport efficiency and a lower vulnerability to cold and drought^{5,6} (Fig. 1a, Supplementary Table 4). By contrast, large grass leaves can attain high minor and total VLA, VSA, VPA and VVA independently of leaf size, which enables high transport efficiency for competition in sunny, moist climates. The model also predicts that C₃ and C₄ species will converge in their vein scaling. C₄ grasses have a higher total VLA, providing a large vein bundle-sheath compartment for concentrating CO₂ to enable high rates of photosynthetic assimilation^{15–17}. We hypothesized that the high total VLA of C₄ grasses arises from minor VLA, and is therefore independent of leaf area.

To test these predictions, we compared the measured scaling relationships of 27 grass species in a common garden against null expectations from the developmental model and against geometric scaling^{5,13} (Extended Data Fig. 1, Supplementary Table 3), and assessed whether developmental scaling would confer small leaves with potential climatic advantages.

Relationship of leaf size with climate

Globally, grasses vary by more than 625-fold, 275-fold and 160,000-fold in leaf length, width and area, respectively^{8,18}, and smaller leaves are associated with cooler and drier climates (Fig. 1b, c, Supplementary Tables 1, 2, 7). We found that, across species, leaf length, width and area were interrelated and that all of these were positively correlated with mean annual temperature, mean annual precipitation and the aridity index (for leaf area, $r=0.24–0.31$, $P<0.0001$; phylogenetic $r=0.08–0.17$, $P<0.0001$) (Fig. 1c, Extended Data Fig. 2, Supplementary Table 7). We found similar relationships with growing season temperature, growing season precipitation and growing season length (Supplementary Table 7). The climatic associations of smaller leaves were independent of plant stature, and statistically similar for C₃ and C₄ species (Supplementary Tables 7, 8). The size of grass leaves was associated interactively with climatic temperature and precipitation, whether considered annually or for the growing season (Extended Data Fig. 3, Supplementary Table 8). The climatic distribution of grass leaf size arises at least in part from the exclusion of large-leaved species from dry and cold climates (Extended Data Fig. 4, Supplementary Table 8).

Thermal benefits of small leaf size

We tested three hypotheses for the thermal advantages of small grass leaves in cold and dry climates using heuristic energy-budget modelling^{19,20}. First, small leaves may avoid chilling or overheating damage (a mechanism that explains the global biogeographical trend in eudicotyledon leaf size³). However, 98% of grass species in the global database had leaves smaller than the modelled width thresholds for such damage (8.16 and 4.47 cm for chilling and overheating, respectively³) and among these species leaf size remained associated with climate (Extended Data Fig. 5), which indicates that this mechanism cannot explain the global trend. Second, small leaves—which are better coupled with air temperature—may achieve a higher light-saturated photosynthetic rate or leaf water-use efficiency under cold or dry climates²⁰ (Extended Data Fig. 5, Supplementary Table 9). These benefits were supported by model simulations (especially at slower wind speeds): in comparisons between the 5th and 95th percentile of leaf sizes in our

Article

Table 1 | Parameters for the scaling of vein diameters and VLA with mature leaf dimensions

Trait and vein order ^a	Scaling with leaf length				Scaling with leaf width				Scaling with leaf area				
	Expected b	r(P)	a	b (95% CI ^b)	Expected b	r(P)	a	b (95% CI)	Expected b	r(P)	a	b (95% CI)	
VD ^c	1 ^{od}	0 < b < 1; e ^e	0.61 (0.0007)	-1.64	0.368 (0.267, 0.508)	b = 0 ^e	0.25 (0.21)		0 < b < 0.5; e ^e	0.71 (3.0 × 10 ⁻⁵)	-1.52	0.319 (0.24, 0.424)	
	2 ^{od}	0 < b < 1; e ^e	0.76 (3.9 × 10 ⁻⁶)	-1.69	0.363 (0.279, 0.473)	b = 0 ^e	0.003 (0.99)		0 < b < 0.5; e ^e	0.65 (0.0003)	-1.58	0.32 (0.224, 0.44)	
VLA ^f	1 ^{og}	b = 0 ^e	0.36 (0.065)			b = -1.0; i ^g	-1.0 (1.2 × 10 ⁻³⁴)	0.009	-1.01 (-1.03, -0.99)	b = -0.5; i ^g	-0.61 (7.0 × 10 ⁻⁴)	0.943	-0.558 (-0.845, -0.27)
	2 ^{og}	b = 0 ^e	0.36 (0.062)			-1.0 ≤ b < 0; i ^g	-0.82 (1.4 × 10 ⁻⁷)	0.951	-0.616 (-0.769, -0.462)	-0.5 ≤ b < 0; i ^g	-0.46 (0.017)	1.51	-0.313 (-0.555, -0.072)
Total major ^g		b = 0 ^e	0.37 (0.058)			-1 ≤ b < 0; i ^g	-0.87 (3.6 × 10 ⁻⁹)	0.999	-0.67 (-0.805, -0.534)	-0.5 ≤ b < 0; i ^g	-0.49 (0.0090)	1.61	-0.346 (-0.589, -0.104)
3 ^{oh}		0 < b < 1; e	0.34 (0.085)			b = 0 ^e	-0.29 (0.137)		0 < b < 0.5; e	0.02 (0.94)			
4 ^{oh}		0 < b < 1; e	0.3 (0.51)			b = 0 ^e	-0.13 (0.774)		0 < b < 0.5; e	0.02 (0.97)			
5 ^{oh}		b = 0 ^e	-0.33 (0.095)			b = 0	0.57 (0.0020)	0.858	0.273 (0.138, 0.408)	b = 0 ^e	0.32 (0.10)		
Total minor ^h		0 < b < 1; e ^e	0.56 (0.0023)	1.13	0.664 (0.489, 1.05)	b = 0 ^e	-0.36 (0.068)		0 < b < 0.5; e	0.20 (0.33)			
Overall total ^h		0 < b < 1; e ^e	0.57 (0.0018)	1.27	0.619 (0.425, 0.878)	-1 ≤ b < 0; i ^g	-0.56 (0.0025)	1.75	-0.317 (-0.496, -0.138)	b = 0 ^e	0.01 (0.95)		

^a1^o to 5^o denote first- to fifth-order veins.

^bCI, confidence interval.

^cVD, vein diameter (in mm).

^dSmaller leaves are predicted to have smaller major vein diameters, which tend to contain narrower xylem conduits (providing tolerance of embolism in cold and dry climates).

^eThe b values predicted from the developmental model are supported in the experimental data (that is, the scaling relationship across species is either absent when expected, or significant, and the predicted b value is within the 95% confidence intervals of the observed b value).

^fVLA in cm of vein per cm² of leaf area.

^gSmaller leaves are predicted to have higher major VLA, which contributes to high maximum hydraulic and photosynthetic function (potentially mitigating a short growing period, and additionally reducing vulnerability to hydraulic decline in dry conditions).

^hMinor and total VLA are predicted to be decoupled from final leaf size. As these contribute to high maximum hydraulic and photosynthetic function, this independence enables potential adaptation to high resource conditions in both small and large leaves.

Parameters are shown across 27 grass species ($n = 11 C_3$ and 16 C_4 grass species) grown in a common garden. Tolerance of cold or dry climates can be conferred by these vein traits (among others, such as VSA, VPA and VVA (Supplementary Table 10)), as they influence hydraulic capacity and safety, and vascular cost (Supplementary Table 4). Expectations for these across-species scaling relationships were derived from a developmental model that predicts the allometric slope b in the equation $\log(\text{trait}) = \log(a) + b \log(\text{mature leaf length, width or area})$, owing to intrinsic (i) and enabling (e) effects (Supplementary Table 6). Expectations from the alternative, geometric scaling model were also derived and tested (Supplementary Tables 6, 10). Allometric equations were fitted using two-tailed phylogenetic reduced major axis (PRMA) or phylogenetic generalized least squares for the scaling of vein diameter and VLA, respectively, yielding r values and P values, as well as parameters a and b (including 95% confidence intervals for b values).

global database, the smaller leaves had 9–27% higher light-saturated photosynthetic rates and/or water-use efficiencies under cold or dry climates (Supplementary Table 9). Third, smaller leaves may mitigate the short daily and/or seasonal growth period that is associated with cold and dry regions with a higher light-saturated photosynthetic rate under warm and moist conditions⁴. This benefit was supported by our simulations (which also showed that smaller leaves had higher transpiration rates) (Supplementary Table 9).

Developmental scaling of grass venation

Developmental vein scaling results in a strong association between vein traits and grass leaf size. As predicted, at a global scale, smaller-leaved species had higher major VLA ($r = -0.84$ to -0.75 , $P < 0.001$) (Fig. 1d, Extended Data Fig. 6). For the 27 grass species that were grown in our common garden, developmental scaling was supported over the null hypothesis of geometric scaling for numerous vein traits (91 versus 27 of the 111 scaling predictions; $P < 0.001$, proportion test) (Table 1, Fig. 2, Extended Data Figs. 6, 7, Supplementary Tables 10, 11). The diameters

of first-order and second-order veins scaled positively with leaf length and area ($b = 0.32$ – 0.37 , $r = 0.61$ – 0.76 , $P < 0.001$) (Fig. 2, Extended Data Fig. 6), and the diameters of xylem conduits scaled with their vein diameters ($b = 1.3$ – 1.5 , $r = 0.48$ – 0.65 , $P < 0.05$ – 0.001) (Extended Data Fig. 6). The VLA of the first-order vein decreased geometrically with increasing leaf width and area ($b = -1.0$ and -0.56 , and $r = -1.00$ and -0.61 , respectively, $P < 0.001$), whereas the VLA of second-order veins decreased less steeply ($b = -0.62$ and -0.31 , and $r = -0.82$ and -0.46 , respectively, $P < 0.05$) (Fig. 2, Extended Data Fig. 6), and the major and total VLA scaled negatively with leaf width ($b = -0.67$ and -0.32 , and $r = -0.87$ and -0.56 , respectively, $P < 0.01$). The diameters of minor veins were independent of leaf length, width and area. The trends of the VLA of third-order and fourth-order veins with leaf length were not significant, but their sum (the total minor VLA) scaled positively with leaf length ($b = 0.35$ – 0.36 , $r = 0.56$ – 0.57 , $P < 0.01$) and was independent of leaf width and area. The VSA, VPA and VVA also scaled positively with leaf length, and negatively with leaf width (with the exception of the VVA of third-order veins), and all were independent of leaf area (Extended Data Fig. 7). We found trends for the fifth-order veins not anticipated

Box 1

Synthetic model of vein development in grass leaves

This model is based on published data for 20 species of grass (Supplementary Tables, 5, 6), and shows how traits that are advantageous under cold and dry climates develop in small leaves. The development of leaves in grasses includes five phases that are based on developmental zones.

Formation and expansion of the primordium (phase P)

'Founder cells' in the periphery of the shoot apical meristem generate the leaf primordium. Cell divisions drive the growth of a hood-like structure, in which the central first-order vein (midvein) and the large second-order veins are initiated early and extend acropetally, which enables their prolonged diameter growth (Box 1 Fig. a, c, e). After this, discrete spatial growth zones develop at the leaf base and drive leaf expansion laterally and longitudinally.

Formation of the cell division zone (phase D)

The basal cell division zone expands slightly, driving minimal growth (Box 1 Fig. a, b). The first- and parallel second-order vein (major veins) complete their patterning basipetally along the leaf blade and increase in diameter (Box 1 Fig. c, e). Meanwhile, beginning at the lamina tip, C_3 species form a single order of small parallel longitudinal minor veins (that is, third-order veins) as do most C_4 species (which we refer to as C_{4-3L} species). Some

C_4 species of the subfamily Panicoideae additionally form smaller parallel fourth-order veins (which we refer to as C_{4-4L} species¹⁵) (Box 1 Fig. c).

Division zone, and formation of the expansion zone (phase D–E)

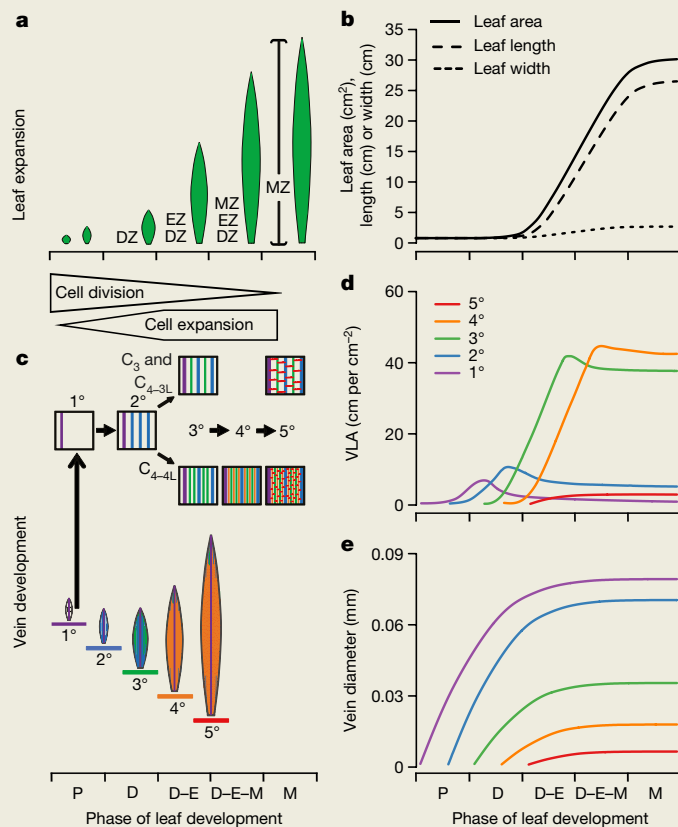
Cells from the division zone transition to a distinct, distal expansion zone. In the expansion zone, cell expansion in width and length spaces apart the first- and second-order veins, resulting in the declines in their VLA (Box 1 Fig. a, b, d). Additional third-order veins (and in some species, fourth-order veins) continue to initiate at the leaf tip between major vein orders and extend basipetally (Box 1 Fig. c–e). The transverse fifth-order veins form last, connecting the longitudinal veins.

Division zone, expansion zone and maturation zone (phase D–E–M)

Cells from the expansion zone mature distally to generate the maturation zone, which increases in size as cells move through the developmental zones (Box 1 Fig. a). The xylem, phloem and bundle sheath of the veins mature.

All of the leaf is in the maturation zone (phase M)

Leaf development is complete, and all cells are differentiated and expanded (Box 1 Fig. a, b).



Box 1 Fig. | Synthetic model for grass leaf ontogeny that predicts developmentally based scaling of vein traits with final leaf size across species.

Processes are plotted against developmental phases: phases P and D refer to the formation of the leaf primordium and the cell division zone (DZ) at the base of the leaf, respectively; phases D–E and D–E–M describe additions of the expansion zone (EZ) and the maturation zone (MZ), respectively; and

phase M denotes the maturation of the whole leaf blade. **a**, Leaf expansion and the formation of zones. **b**, Increases in leaf length, width and area.

c, Patterning of leaf vein orders from first-order veins to fifth-order transverse veins for C_3 and C_4 species; some C_4 species develop fourth-order longitudinal veins (C_{4-4L} species), whereas C_3 species and C_{4-3L} species do not. **d, e**, Increases in VLA (**d**) and vein diameter (**e**) for each vein order.

by the developmental model, being positive scaling of their VLA, VSA and VPA with leaf width ($r=0.46\text{--}0.57, P<0.05$).

C_3 and C_4 grasses converged in vein scaling (Fig. 2, Extended Data Fig. 8, Supplementary Table 3). C_4 species had more numerous, narrower third-order veins with higher VLA, VSA and VPA, and 7 out of 16 C_4 species had fourth-order veins; this resulted in the C_4 species having, on average, almost double the total VLA of the C_3 species. The C_4 species also had narrower fifth-order veins with lower VSA, VPA and VVA ($P=0.001\text{--}0.05$).

Hydraulic benefits of small leaf size

Across the 27 grass species that we grew experimentally, a number of key vein traits were related to the native climates of the species. Small leaf size and higher major VLA, VSA, VPA and VVA were associated with lower mean annual and growing season precipitation, a lower aridity index and a shorter growing season (Supplementary Table 7). Furthermore, our tests supported assumptions based on the published literature (which is collated in Supplementary Table 4) that C_3 grasses adapted to colder or drier climates have higher light-saturated photosynthetic rates in moist soil, which are associated with their major vein traits (Extended Data Fig. 9).

Developmental scaling contributes mechanistically to climate adaptation globally. Vein scaling can explain the absence of leaves larger than 51.4 cm² in areas in which the mean annual temperatures are below 0 °C (Extended Data Fig. 5), as the midrib conduits of leaves larger than this would be wider than 35 µm (Extended Data Fig. 6) and thus vulnerable to freeze-thaw embolism²¹. Additionally, the narrow xylem conduits of small leaves resist embolism during drought, and their higher major VLA provides a high capacity flow around blockages, which further reduces hydraulic vulnerability to dehydration^{6,22–25} (Supplementary Table 4). The higher major VLA of smaller leaves also contributes to mitigating the shorter growing periods that are associated with colder, drier climates^{11,12} by providing higher hydraulic conductance, which enables the maintenance of open stomata for higher photosynthetic rates despite the higher transpiration loads expected from their thinner boundary layer^{6,26} (Extended Data Fig. 9).

Discussion

The worldwide association of small leaf size in grasses with cold and arid climates arises from millions of years of grass migration and evolution, from the tropics to colder, drier climates and from forest understoreys to open grasslands⁹ (Supplementary Table 1). The biophysical and developmental advantages of small leaves can explain this pattern. The thinner boundary layer of small grass leaves confers a moderately higher photosynthetic rate and water-use efficiency in cold and dry climates, and can partially mitigate shorter growing days and seasons (especially under the very low wind speeds that are expected for closed, dense stands)^{27–30}. The higher major VLA and narrower xylem conduits of these smaller leaves directly contribute to cold and drought tolerance. The strong climatic association of leaf size and vein traits indicates their substantial importance to plant adaptation against a background of other features—including leaf hairs, leaf rolling and mesophyll desiccation tolerance, and (beyond leaves) annual versus perennial life history, stem and root hydraulic adaptation, and root morphology—that help plants to cope with climatic pressures^{31–33}.

Developmentally based vein scaling relationships held strongly across diverse grass species—even including those species (such as bamboos) that possess a pseudopetiole. These relationships may also apply to nongrass species from other families within the Poales. Developmental vein scaling relationships in grass leaves are distinct from, though analogous to, those of typical eudicotyledon leaves (Figs. 1, 2, Box 1). In eudicotyledons (as expected from their diffuse lamina growth), major vein traits scale negatively with final leaf area (Supplementary

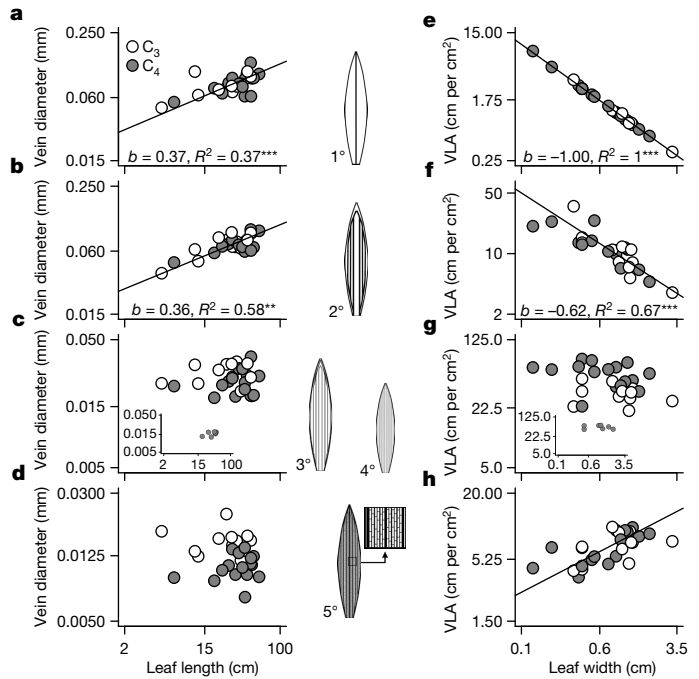


Fig. 2 | The scaling of vein traits with leaf dimensions for 27 species of grass grown in a common garden. $n=11$ C_3 (shown as white points) and 16 C_4 (shown as grey points) grass species. **a–d**, Relationship of vein diameters with leaf length. **e–h**, Relationship of VLA with leaf width. In **a**, **e**, relationships are shown for first-order veins; in **b**, **f**, for second-order veins; in **c**, **g**, for third-order veins (inset panels show fourth-order veins for the species that possess them); and in **d**, **h**, fifth-order transverse veins. Each point represents the mean value of a species. PRMA or phylogenetic generalized least square regressions were fitted for $\log(\text{vein diameter or VLA}) = \log(a) + b \log(\text{leaf length or width})$, respectively. Parameters and the goodness of fit are given in Table 1, Supplementary Table 10. $**P<0.01$, $***P<0.001$. $P=0.0007$ (a), 3.9×10^{-6} (b), 1.2×10^{-34} (e), 1.4×10^{-7} (f) and 0.0020 (h) (all two-tailed). Significant trends are plotted with PRMA. Supplementary Table 3 gives the s.e. for species trait values.

Table 4), whereas in grasses vein traits scale more directly with length or width (Table 1, Fig. 2, Box 1). However, for both grasses and eudicotyledons, total VLA—which is a key determinant of hydraulic capacity and photosynthetic rate⁶—was independent of final leaf area. This lack of constraint on total VLA would enable grass diversification in leaf size across environments, as for eudicotyledons^{5,26,34}: large-leaved grasses, despite their low major VLA, can achieve sufficient hydraulic capacity with their minor vein length to occupy wet, sunny habitats^{6,34,35}. The decoupling of total VLA from leaf size also enables C_4 species to achieve, on average, a higher VLA than that of C_3 species, irrespective of leaf size (Fig. 2, Box 1). Unlike in eudicotyledons⁵, larger leaves in grasses did not have a higher VVA (which contributes substantially to the cost of leaf construction³⁶); this indicates that there is less restriction on the evolution of grass leaf size in resource-rich environments, in which larger leaves may confer advantages in light-use efficiency and by shading other species^{37,38}. Although the common developmental program across grass species explains many vein scaling relationships, these relationships may also arise from selection on the basis of function. In longer leaves, larger-diameter veins may provide necessary structural and hydraulic support^{6,39}. In wider leaves, more numerous fifth-order transverse veins may reinforce the grass leaves against bending⁴⁰ and provide hydraulic pathways that mitigate their lower major VLA⁶. Similarly, the greater diameters of fifth-order veins in C_3 species than in C_4 species may compensate for their lower minor VLA (Fig. 2).

The relationships among grass leaf size, vein traits and climate have diverse potential applications. In eudicotyledons, these traits

are frequently included for estimating the adaptation of species to climate⁶, an approach that can now be extended to grasses. For grasses (as shown for eudicotyledons^{5,41}), vein scaling can enable the reconstruction of leaf size from fossilized leaf fragments, to improve palaeoclimate reconstructions (Extended Data Fig. 10). Anticipating future climate change, leaf size and vein traits represent key targets for the design of grass crops, which are central to food and biofuel security^{42,43}. A current grand challenge is the engineering of C₄ metabolism into C₃ crops such as rice⁴³, and introducing a higher total VLA has been targeted as a promising step^{44,45}. Global trends indicate that C₄ species with narrow leaves and high major VLA would be especially advantaged under the increased temperature and irregular precipitation that are expected for grasslands in scenarios of global climate change^{25,46,47}.

Online content

Any methods, additional references, Nature Research reporting summaries, source data, extended data, supplementary information, acknowledgements, peer review information; details of author contributions and competing interests; and statements of data and code availability are available at <https://doi.org/10.1038/s41586-021-03370-0>.

1. Hort, A. *Enquiry into Plants, Vol. I*, by Theophrastus (Harvard Univ. Press, 1948).
2. Peppe, D. J. et al. Sensitivity of leaf size and shape to climate: global patterns and paleoclimatic applications. *New Phytol.* **190**, 724–739 (2011).
3. Wright, I. J. et al. Global climatic drivers of leaf size. *Science* **357**, 917–921 (2017).
4. Gates, D. M. Transpiration and leaf temperature. *Annu. Rev. Plant Physiol.* **19**, 211–238 (1968).
5. Sack, L. et al. Developmentally based scaling of leaf venation architecture explains global ecological patterns. *Nat. Commun.* **3**, 837 (2012).
6. Sack, L. & Scoffoni, C. Leaf venation: structure, function, development, evolution, ecology and applications in the past, present and future. *New Phytol.* **198**, 983–1000 (2013).
7. Beer, C. et al. Terrestrial gross carbon dioxide uptake: global distribution and covariation with climate. *Science* **329**, 834–838 (2010).
8. Gallaher, T. J. et al. Leaf shape and size track habitat transitions across forest–grassland boundaries in the grass family (Poaceae). *Evolution* **73**, 927–946 (2019).
9. Soreng, R. J. et al. A worldwide phylogenetic classification of the Poaceae (Gramineae) II: an update and a comparison of two 2015 classifications. *J. Syst. Evol.* **55**, 259–290 (2017).
10. Schuepp, P. H. Tansley review no. 59 leaf boundary layers. *New Phytol.* **125**, 477–507 (1993).
11. Orians, G. H. & Solbrig, O. T. A cost–income model of leaves and roots with special reference to arid and semiarid areas. *Am. Nat.* **111**, 677–690 (1977).
12. Körner, C. Plant adaptation to cold climates. *F1000Res.* **5**, 2769 (2016).
13. Niklas, K. J. *Plant Allometry: The Scaling of Form and Process* (Univ. Chicago Press, 1994).
14. Nelson, T. & Dengler, N. Leaf vascular pattern formation. *Plant Cell* **9**, 1121–1135 (1997).
15. Christin, P. A. et al. Anatomical enablers and the evolution of C₄ photosynthesis in grasses. *Proc. Natl Acad. Sci. USA* **110**, 1381–1386 (2013).
16. Ueno, O., Kawano, Y., Wakayama, M. & Takeda, T. Leaf vascular systems in C₃ and C₄ grasses: a two-dimensional analysis. *Ann. Bot.* **97**, 611–621 (2006).
17. Sage, R. F. The evolution of C₄ photosynthesis. *New Phytol.* **161**, 341–370 (2004).
18. Clayton, W. D., Vorontsova, M. S., Harman, K. T. & Williamson, H. *GrassBase—The Online World Grass Flora* <http://www.kew.org/data/grasses-db.html> (2006).
19. Parkhurst, D. F. & Loucks, O. L. Optimal leaf size in relation to environment. *J. Ecol.* **60**, 505–537 (1972).
20. Okajima, Y., Taneda, H., Noguchi, K. & Terashima, I. Optimum leaf size predicted by a novel leaf energy balance model incorporating dependencies of photosynthesis on light and temperature. *Ecol. Res.* **27**, 333–346 (2012).
21. Davis, S. D., Sperry, J. S. & Hacke, U. G. The relationship between xylem conduit diameter and cavitation caused by freezing. *Am. J. Bot.* **86**, 1367–1372 (1999).
22. Blackman, C. J., Brodribb, T. J. & Jordan, G. J. Leaf hydraulic vulnerability is related to conduit dimensions and drought resistance across a diverse range of woody angiosperms. *New Phytol.* **188**, 1113–1123 (2010).
23. Scoffoni, C., Rawls, M., McKown, A., Cochard, H. & Sack, L. Decline of leaf hydraulic conductance with dehydration: relationship to leaf size and venation architecture. *Plant Physiol.* **156**, 832–843 (2011).
24. Scoffoni, C. et al. Leaf vein xylem conduit diameter influences susceptibility to embolism and hydraulic decline. *New Phytol.* **213**, 1076–1092 (2017).
25. Craine, J. M. et al. Global diversity of drought tolerance and grassland climate-change resilience. *Nat. Clim. Chang.* **3**, 63–67 (2013).
26. Scoffoni, C. et al. Hydraulic basis for the evolution of photosynthetic productivity. *Nat. Plants* **2**, 16072 (2016).
27. Jones, H. G. *Plants and Microclimate: A Quantitative Approach to Environmental Plant Physiology* 3rd edn (Cambridge Univ. Press, 2014).
28. Grace, J. *Plant–Atmosphere Relationships* 1st edn (Chapman and Hall, 1983).
29. Weiser, R. L., Asrar, G., Miller, G. P. & Kanemasu, E. T. Assessing grassland biophysical characteristics from spectral measurements. *Remote Sens. Environ.* **20**, 141–152 (1986).
30. Meinzer, F. C. & Grantz, D. A. Stomatal control of transpiration from a developing sugarcane canopy. *Plant Cell Environ.* **12**, 635–642 (1989).
31. Liu, H. et al. Life history is a key factor explaining functional trait diversity among subtropical grasses, and its influence differs between C₃ and C₄ species. *J. Exp. Bot.* **70**, 1567–1580 (2019).
32. Fort, F., Jouany, C. & Cruz, P. Root and leaf functional trait relations in Poaceae species: Implications of differing resource-acquisition strategies. *J. Plant Ecol.* **6**, 211–219 (2013).
33. Holloway-Phillips, M. M. & Brodribb, T. J. Contrasting hydraulic regulation in closely related forage grasses: implications for plant water use. *Funct. Plant Biol.* **38**, 594–605 (2011).
34. Brodribb, T. J., Feild, T. S. & Sack, L. Viewing leaf structure and evolution from a hydraulic perspective. *Funct. Plant Biol.* **37**, 488–498 (2010).
35. Linacre, E. T. Further notes on a feature of leaf and air temperatures. *Archiv Meteorol. Geophys. Bioklimatol. B* **15**, 422–436 (1967).
36. John, G. P. et al. The anatomical and compositional basis of leaf mass per area. *Ecol. Lett.* **20**, 412–425 (2017).
37. Givnish, T. J. Comparative studies of leaf form: assessing the relative roles of selective pressures and phylogenetic constraints. *New Phytol.* **106**, 131–160 (1987).
38. Lusk, C. H., Grierson, E. R. P. & Laughlin, D. C. Large leaves in warm, moist environments confer an advantage in seedling light interception efficiency. *New Phytol.* **223**, 1319–1327 (2019).
39. Olson, M. E. et al. Plant height and hydraulic vulnerability to drought and cold. *Proc. Natl Acad. Sci. USA* **115**, 7551–7556 (2018).
40. Niklas, K. J. A mechanical perspective on foliage leaf form and function. *New Phytol.* **143**, 19–31 (1999).
41. Merkhofer, L. et al. Resolving Australian analogs for an Eocene Patagonian paleorainforest using leaf size and floristics. *Am. J. Bot.* **102**, 1160–1173 (2015).
42. Somerville, C. The billion-ton biofuels vision. *Science* **312**, 1277 (2006).
43. Sedelnikova, O. V., Hughes, T. E. & Langdale, J. A. Understanding the genetic basis of C₄ kranz anatomy with a view to engineering C₃ crops. *Annu. Rev. Genet.* **52**, 249–270 (2018).
44. Sage, R. F. & Zhu, X. G. Exploiting the engine of C₄ photosynthesis. *J. Exp. Bot.* **62**, 2989–3000 (2011).
45. Feldman, A. B. et al. Increasing leaf vein density via mutagenesis in rice results in an enhanced rate of photosynthesis, smaller cell sizes and can reduce interveinal mesophyll cell number. *Front. Plant Sci.* **8**, 1883 (2017).
46. Edwards, E. J. et al. The origins of C₄ grasslands: integrating evolutionary and ecosystem science. *Science* **328**, 587–591 (2010).
47. Linder, H. P., Lehmann, C. E. R., Archibald, S., Osborne, C. P. & Richardson, D. M. Global grass (Poaceae) success underpinned by traits facilitating colonization, persistence and habitat transformation. *Biol. Rev. Camb. Philos. Soc.* **93**, 1125–1144 (2018).

Publisher's note Springer Nature remains neutral with regard to jurisdictional claims in published maps and institutional affiliations.

© The Author(s), under exclusive licence to Springer Nature Limited 2021

Article

Methods

No statistical methods were used to predetermine sample size. Investigators were not blinded to allocation during experiments and outcome assessment.

Testing for the linkage of leaf size and vein traits with climate across grass species worldwide

We extracted data from the Kew Royal Botanic Garden Grassbase, which was compiled from a combination of floristic accounts and publications¹⁸. We extracted all available data for maximum leaf length, maximum leaf width, maximum second-order vein number and maximum culm height data, which included values for up to 1,752 species depending on the trait (that is, up to 912 C₃ and 840 C₄ species from 373 genera)¹⁸. We calculated leaf area by multiplying maximum leaf length by maximum leaf width. We divided the maximum leaf length and maximum second-order vein number, respectively, by maximum leaf width to determine the VLA of first- and second-order veins, and summed these to calculate the major VLA, resulting in values for 616 species for these traits. To test associations of leaf morphological and venation traits with the native climates of the species, we extracted geographical records from the Global Biodiversity Information Facility web portal (<http://www.gbif.org>). The names of species were checked against the Kew grass synonymy database¹⁸ via the software package Taxonome⁴⁸ and The Plant List (<http://www.theplantlist.org>) using the package Taxostand in R⁴⁹. We discarded records if these were duplicates, the names were not recognized in any databases, the country did not match the coordinates, the coordinates contained fewer than three decimals or species had fewer than five occurrences. For each location, values for mean annual temperature (MAT), mean annual precipitation (MAP) and mean monthly temperature and precipitation were extracted from WorldClim2.5-arc minute resolution⁵⁰; values for the aridity index⁵¹ were from CRU TS4.01 01⁵². We also estimated growing season variables, considering growing season months as those with mean temperature $\geq 4^{\circ}\text{C}$ and precipitation $\geq 2 \times$ the mean monthly temperature; growing season length was calculated as the number of months that fulfilled these criteria, growing season temperature was calculated by averaging the mean temperatures of these months, and growing season precipitation was calculated by summing their mean precipitation⁵³. Climate variables were averaged from all given locations for each species. We focused on the relationships of traits with mean climate variables based on the hypothesis that, if gene flow occurs among populations of a given species across its native range, then the mean phenotypic trait values of this species will be related to their mean climate variables⁵⁴.

Construction of a synthetic model for grass leaf development, and derivation of allometric predictions based on developmental and geometric scaling

To determine whether leaf development constrains specific vein traits in smaller leaves, we formulated a synthetic grass leaf developmental model and derived expectations for the relationship of vein traits with final leaf dimensions across species (Box 1, Supplementary Tables 5, 6). To construct this model, we conducted searches for previously published studies that included developmental data and/or images of grass leaf development using the keywords 'grass leaf development', 'grass vein development', 'grass histogenesis', 'grass morphogenesis', 'Poaceae', 'leaf ontogeny', 'leaf histology', 'leaf growth', 'leaf anatomy', 'vascular development' and 'vasculature development' in the Web of Science database and Google Scholar search engine, resulting in a compilation of 61 studies of 20 grass species^{14,55–114}. From these studies, we extracted the key steps in leaf and vein development that were general across species into a synthetic model. Then, given the spatial and temporal constraints arising from development according to this model, we derived expectations for the scaling across species of vein traits with mature leaf size. For instance, the VLA of first-order veins declines

geometrically with final leaf width ($1^{\circ}\text{ VLA} = 1/\text{leaf width}$) as veins are separated by greater numbers of cell divisions and/or by larger cells. By contrast, the VLA of second-order veins declines less steeply than geometrically with final leaf width, as wider leaves may form greater numbers of second-order veins (though these will be spaced further apart by subsequent leaf expansion); Box 1 and Supplementary Table 6 provide additional derivations.

Further, as a null hypothesis against which to test developmentally based scaling predictions, we derived expectations for the relationships of vein traits to leaf dimensions on the basis of geometric scaling^{5,13}. Geometric scaling represents the relationships expected among the dimensions of an object given increases in size, while maintaining constant proportions and composition. Thus, dimensions such as length (L), area (A) and volume (V) would be inter-related as $A \propto L^2$ and $V \propto L^3$. Predictions can then be derived for any other traits on the basis of their dimensions. For instance, given geometric scaling, VLA would be expected to scale with leaf width as $\text{VLA} \propto LW^{-1}$, because VLA (as a linear dimension divided by an area (that is, L/A)) would be related to $L/L^2=L^{-1}$, whereas LW would scale directly with L . In total, we compared 111 predictions derived from the developmental model to respective predictions from geometric scaling. These 111 predictions included the scaling relationships of five vein diameters (that is, for each of five vein orders) versus three leaf dimensions (that is, leaf length, width and area), amounting to 15 predictions, plus the scaling relationships for VLA, VSA, VPA and VVA for each of the five vein orders, for the major veins, minor veins, and the total vein systems, versus the three leaf dimensions (amounting to $4 \times 8 \times 3 = 96$ predictions). The developmental model predictions for relationships generally differed strongly from those of geometric scaling (that is, 75% of predictions differed), although—for a few relationships, such as that of the VLA of first-order veins with final leaf size—the expectations from developmental scaling and geometric scaling were the same. Overall, developmental scaling predicted that 51 vein traits would scale with leaf size and 60 traits would be independent of leaf dimensions, whereas geometric scaling predicted 63 and 48, respectively (Supplementary Tables 6, 10).

Plant material

To test vein scaling relationships, we grew grasses of 27 diverse species in a common garden to reduce the environmentally induced plasticity that would occur in wild plants in their native ranges (Extended Data Fig. 2, Supplementary Table 3). Although experimental species were selected to encompass large phylogenetic and functional variation (including 11 C₃ species and 16 C₄ species that represented 11 independent C₄ origins), the species necessarily included a only subset of the phylogenetic distribution of the 1,752 species in the database analyses of global trait–climate relationships. Seeds were acquired from seed banks and commercial sources (Supplementary Table 3). Before germination, seeds were surface-sterilized with 10% NaClO and 0.1% Triton X-100 detergent, rinsed three times with sterile water and finally sown on plates of 0.8% agar sealed with Micropore surgical tape (3M). Seeds were germinated in chambers maintained at 26 °C, under moderate-intensity cool white fluorescent lighting with a 12-h photoperiod. When roots were 2–3 cm long, seedlings were transplanted to 3.6-l pots with potting soil (1:1:1.5:1.5:3 of coarse vermiculite:perlite:washed plaster sand:sandy loam:peat moss).

Plants were grown at the UCLA Plant Growth Center (minimum, mean and maximum daily values for temperature, 20.1, 23.4 and 34.0 °C; for relative humidity, 28, 50 and 65%; and mean and maximum photosynthetically active radiation during daylight period, 107 and 1,988 μmol photons m⁻² s⁻¹ (HOBO Micro Station with Smart Sensors, Onset)), arranged in 6 randomized blocks spread over 3 benches, with 1 individual per species per block and 2 blocks per bench ($n=6$, except $n=4$ for *Alloteropsis semialata*). Plants were irrigated daily with water containing fertilizer (200–250 ppm of 20:20:20 N:P:K, Scotts Peters Professional water soluble fertilizer, Everris International B.V.). All species were grown until flowering to confirm the identities of the species.

Sample anatomical preparation

Leaves were collected when plants had numerous mature leaves, after 2.5–7 months of growth, depending on species (given variation in growth rates). Leaves from each of 6 individuals per species were fixed and stored in FAA solution (37% formaldehyde–glacial acetic acid, 95% ethanol in deionized water). Transverse sections were made for one leaf from each of three individuals. Rectangular samples were cut from the centre of leaves halfway along the length of the blade and gradually infiltrated under vacuum with low viscosity acrylic resin for one week (L. R. White; London Resin), and set in resin in gelatin capsules to dry at 55 °C overnight. Transverse cross-sections of 1 µm in thickness were prepared using glass knives (LKB 7800 KnifeMaker, LKB Produkter) in a rotary microtome (Leica Ultracut E, Reichert-Jung), placed on slides, and stained with 0.01% toluidine blue in 1% sodium borate (w/v). Slides were imaged with a light microscope using 5×, 20× and 40× objectives (Leica Lietz DMRB; Leica Microsystems) and a camera with imaging software (SPOT Imaging Solution, Diagnostic Instruments). Additionally, one leaf from each of three individuals was used to prepare chemically cleared leaf sections to visualize veins. Square sections of 1 cm × 1 cm were cut from the centre of the leaf at the widest point, cleared with 5% NaOH in ethanol, stained with safranin and counterstained with fast-green¹¹⁵. Sections were mounted with water in transparency film (CG5000; 3M Visual Systems Division) and scanned (flatbed scanner; Canon Scan Lide 90; 1,200 dots per inch), and further imaged with a light microscope using 5× and 10× objectives.

Quantification of leaf dimensions and vein traits

The leaf dimensions tested were leaf width, leaf length and leaf area, with leaf width and leaf length measured at the widest and longest regions of the leaf, respectively. Leaf area was calculated as leaf length × leaf width^{116–118}. Estimates of leaf area from length and width can be improved by multiplying by a constant correction factor, which has been proposed as 0.7–0.9 for grasses^{116–118}; however, as there is no standard value we did not apply such a correction factor. Applying a constant correction factor would have no influence on correlations or regression fits or their statistical significance for trait–climate relationships. Further, applying a constant correction factor would not influence the tests of scaling of vein traits with leaf area, which focused on power-law scaling exponents; multiplying estimates of leaf area by a constant would result only in a change to the power-law scaling intercept, and not the exponent. Thus, applying a correction factor to leaf area or not would have no influence on any of the findings of our study.

We measured and analysed cross-sections of one leaf for each of three individuals per species, to quantify the diameters and numbers of veins in the transverse plane for all vein orders (excluding fifth-order veins, which generally were not visible in transverse sections and for which we used the chemically cleared and stained leaf sections). Vein orders were established for each species on the basis of vein size, presence or absence of enlarged metaxylem and presence or absence of fibrous tissue above or below the vein^{119,120}. The first-order vein (midvein) was the large central vein containing the largest metaxylem and fibrous tissue, and the second-order veins were the ‘large’ veins that were substantially smaller than the midvein and of similar structure. We identified the minor veins as the smaller veins (that is, the third-order ‘intermediate’ and fourth-order ‘small’ veins, and perpendicular fifth-order transverse veins)¹²⁰. Notably, fourth-order veins occur only in NADP-ME C₄ grasses of the subfamily Panicoideae (7 out of the 16 of the C₄ species we grew)¹⁵, and can be distinguished on the basis of their smaller overall size than third-order veins and their absence of sclerenchyma strands. For the species *Lasiacis sorghoidea*, second-order veins were too few to be counted in our prepared transverse sections, and we established vein orders and quantified associated traits using the chemically cleared and stained leaves.

For each vein order, VLA was quantified as the vein number per leaf width (per cm or per mm), which is equivalent to VLA (same units), assuming an approximately rectangular leaf. Cross-sectional vein diameters (VD) were measured excluding the bundle and mesome sheath cell layers, and averaging horizontal and vertical axes. Cross-sectional diameters were measured for all xylem conduits in each vein order by considering the lumen cross-sections as ellipses and averaging the major and minor axes. We categorized two metaxylem types within major veins on the basis of their highly distinct sizes (that is, large and small metaxylem), and one metaxylem type for minor veins (that is, small metaxylem). We focused on the large metaxylem conduits within major veins in calculating average conduit diameter values, as these would contribute the bulk of maximum flow^{121,122}. For *L. sorghoidea*, as second-order veins were too few to be counted from our prepared transverse sections, we could not quantify the conduits within these veins and thus analyses of second-order vein conduit dimensions excluded this species.

For all vein orders, we estimated VSA, VPA and VVA as VSA = VLA × π × VD; VPA = VLA × VD; and VVA = VLA × π × (VD/2)².

Determining vein allometries and testing against predictions from developmental and geometric scaling

We determined trait scaling relationships by fitting lines to log-transformed data. The relationship of each vein trait (*y*) to a given leaf dimension (*x*) was considered as an allometric power law: $y = ax^b$, $\log(y) = \log(a) + b \log(x)$, in which *b* is the scaling exponent.

We tested these relationships against the predictions from developmentally based scaling derived from the synthetic leaf developmental model (as described in ‘Construction of a synthetic model for grass leaf development, and derivation of allometric predictions based on developmental and geometric scaling’ (Table 1, Box 1, Supplementary Table 6)). A scaling relationship was considered to be consistent with a prediction if its 95% confidence intervals included the predicted slope. We tested whether a greater proportion of predictions were explained by developmental scaling than by geometric scaling using a proportion test (Minitab 16).

Testing assumptions for the linkages of photosynthetic rate with climate and vein traits

For the grass species grown experimentally, light-saturated rates of photosynthesis were measured for plants in moist soil, enabling a test of the assumptions that C₃ grass species from arid or cold environments have high photosynthetic rates, and that photosynthetic rate would be related to VLA and VSA. Light-saturated rates of photosynthesis were measured from 17 February 2010 to 28 June 2010, between 09:00 h and 15:00 h, on a mature leaf on each plant for 6 plants per species. Measurements were taken of steady-state net light-saturated photosynthetic rate per leaf area (<2% change over six minutes) using a LI-6400 XT portable photosynthesis system (LI-COR). Conditions within the leaf chamber were set to 25 °C, with reference CO₂ 400 ppm, photosynthetic photon flux density 2,000 µmol m⁻² s⁻¹, and relative humidity 60–80%, resulting in vapour pressure deficits of 0.80–1.6 kPa. Measurements were made on 1 or 2 leaves from each of 4–6 plants (except *L. sorghoidea* for which 3 leaves from each of 2 plants were used).

In addition, we tested for stronger general support of the relationships of photosynthetic rate with climate variables by combining our data for 8 C₃ terrestrial species with data for 13 Northern Hemisphere temperate terrestrial C₃ grass species from the Global Plant Trait Network (GLO-PNET) database¹²³, for which photosynthesis, latitude and longitude data for their field site were available (Supplementary Table 12). We extracted the climate variables MAT, MAP and monthly temperature and precipitation to calculate growing season length (methods of calculation are described in ‘Testing for the linkage of leaf size and vein traits with climate across grass species worldwide’), on the basis of the latitude and longitude from which each species was measured.

Phylogenetic reconstruction

A phylogenetic hypothesis for the 27 experimentally grown species considered in this study was inferred from three markers from the chloroplast genome (*rbcL*, *ndhF* and *trnKmatK*), available for the exact same accessions in published datasets^{124,125}. Each marker was aligned individually using MUSCLE¹²⁶, and the alignments were manually refined. The total dataset was 6,179-bp long. The program BEAST¹²⁷ was used to obtain a time-calibrated phylogeny under a relaxed clock model with uncorrelated evolutionary rates that follow a log-normal distribution. The substitution model was set to a general time reversible model with a gamma-shape parameter and a proportion of invariants. The root of the tree (split of BOP and PACMAD clades) was forced to follow a normal distribution with a mean of 51.2 million years ago (Ma) and a standard deviation of 0.0001 Ma, on the basis of previous estimates¹²⁸. The addition of phytolith fossils would alter the absolute ages estimated by molecular dating¹²⁹, but the relative ages would remain unchanged and the comparative analyses consequently would be unaffected. Two parallel analyses were run for 10,000,000 generations, sampling a tree every 1,000 generations. Median ages across the 18,000 trees samples of a burn-in period of 1,000,000 generations were mapped on the maximum credibility tree. The burn-in period was largely sufficient for the analysis to reach stability, as verified with the program Tracer (<http://beast.community/tracer>).

Using the R Language and Environment version 3.4.1¹³⁰ with the ape R package¹³¹ a phylogenetic hypothesis for 1,752 of the Grassbase species was extracted from a published phylogeny available through Dryad¹³². The source phylogeny assessed relationships among 3,595 species using a set of 14 subtrees using various genetic datasets in combination with three core plastid markers *rbcL*, *ndhF* and *matK*, with dating based on macrofossil evidence⁹.

Testing trait–climate associations

To test trait–climate associations, we quantified the strength of correlations using Pearson’s *r* rather than fitting specific predictive regression equations with *R*² values. For trait–climate associations, we calculated both ahistorical correlations and relationships accounting for phylogenetic relatedness (phylogenetic generalized least squares (PGLS) or PRMA, as described in ‘Comparative analyses’). Although the phylogenetic analyses more robustly test our evolutionary hypotheses, the ahistorical Pearson’s *r* values better resolve the strengths of existing relationships across species—especially when trends arise from variation among groups that split in evolution deep in the phylogeny¹³³. In both types of analysis, the *r* values provide a conservative estimate of trait–climate relationships. As in previous biogeographical trait–climate analyses^{134,135}, we related the average trait values of a species from a database or experimental measurements to modelled native climates on the basis of natural occurrences; relationships would be stronger if traits and climate were matched for individual plants¹³⁶. Additionally, the modelled native climates do not account for variation in temperature, irradiance and water availability (owing to microclimates associated with topography and canopy cover, or soil characteristics) to which species would be adapted in the field; accounting for this variation would probably improve the strength of trait–climate relationships¹³⁶. Overall, global associations of traits with climate that were supported by substantial, statistically significant ahistorical *r* values indicate robust, biologically important relationships, and significant phylogenetic correlations additionally indicate support for the evolutionary hypotheses^{137,138}.

We implemented several further analyses to resolve the associations of traits with climate in the worldwide grass trait database. We conducted phylogenetic multiple regression to test for significant interactive effects of temperature and precipitation on leaf traits. Models including MAT and MAP (or growing season temperature and growing season precipitation) alone or in combination, and including

an interaction, were compared using the Akaike information criterion¹³⁹. Before phylogenetic multiple regression analyses, MAP values were divided by 50 to achieve a similar scale of values as those for MAT, and growing season precipitation values were divided by 100 to achieve a similar scale of values as for growing season temperature. Plant traits, MAP and MAT were then log-transformed, and MAT and MAP (and growing season temperature and growing season precipitation) were centred by subtracting the mean to render coefficients of main effects and interaction terms biologically interpretable¹⁴⁰.

The parametric correlation and regression statistics calculated in this study are subject to assumptions (that is, the independence of observations, and the normal distribution and homoscedasticity of residuals)¹⁴¹. Evolutionary nonindependence among species was adjusted for using phylogenetic statistics¹³³. To check that the assumptions of normality and heteroscedasticity did not influence statistical significance of univariate analyses, we checked for significance of Spearman’s rank correlations, which are not subject to these assumptions, and confirmed as significant (*P*<0.05) the relationships presented in the Article. For the multiple regression of leaf area versus MAT and MAP in the 1,752-species global database, the 29 species with MAT<0 °C resulted in a left-skew of log-transformed MAT and a notable heteroscedasticity of residuals (Supplementary Fig. 1). To confirm that this skew did not influence the findings of the multiple regressions, we repeated the analysis excluding the 29 species, which alleviated the skew and heteroscedasticity (Supplementary Fig. 2); the key finding of the multiple regression analysis (that is, the interactive effect of MAT and MAP) was unaffected (Supplementary Table 8). Notably, the multiple regression analysis of leaf area versus growing season temperature and growing season precipitation also confirmed the trend, with greater normality and homoscedasticity of residuals, both when including all 1,752 species and when excluding the 29 species with MAT<0 °C (Supplementary Tables 7, 8, Supplementary Figs. 3, 4).

We conducted hierarchical partitioning analyses on log-transformed data to resolve the independent statistical associations of leaf size with individual climate variables¹⁴². Finally, we distinguished whether trait–climate correlations can be partially explained owing to ‘triangular relationships’ (that is, when data are missing in one or more corners of the plot, an analysis that can provide special insights)^{143,144}. For example, a positive trait–climate correlation would arise at least in part from a triangular relationship if high trait values are few or absent at lower values of the climate variable, or if low trait values are few or absent at high values of the climate variable. To test for the presence of triangular relationships, we implemented quantile regression analyses, determining regression slopes fitted through the 5%, 50% and 95% quantiles of log-transformed data^{145–147}. A triangular relationship was supported when the regressions through the 95% and 5% quantiles differed according to *t*-tests.

Comparative analyses

Comparative phylogenetic statistical analyses accounting for the effects of phylogenetic covariance on trait–climate and trait–trait relationships were conducted using the R Language and Environment version 3.4.1¹³⁰.

Regression coefficients were estimated using PGLS and/or PRMA, in each case basing the phylogenetic correction on Pagel’s λ ^{148,149} estimated by maximum likelihood¹⁵⁰. For PGLS, corPagel¹⁵¹ was used in combination with gls¹⁵⁰ and optimized¹³¹ to establish maximum likelihood estimates of λ in the 0–1 range; for PRMA, phyl.RMA¹⁵¹ was used. Confidence intervals for *b* estimated using PRMA were determined following previous work¹⁵²:

$$\pm \hat{b}(\sqrt{B+1} \pm \sqrt{B}), \text{ in which } B = \frac{1-r^2}{N-2} f_{1-\alpha, 1, n-2}$$

in which \hat{b} is the fitted value for *b*; *r* is a correlation coefficient, for which we used a phylogenetically corrected estimate based on the

variance–covariance matrix output by phyl.RMA; n is the number of pairs of observations; and $f_{1-\alpha, n-2}$ is the critical value from the f distribution.

Differences in species-level trait means between C₃ and C₄ species were tested using a phylogenetically corrected analysis of variance (ANOVA), both parametric (based on PGLS) and nonparametric¹⁵³ using the phyloANOVA R package¹⁵¹.

The effect of phylogenetic corrections was evaluated by comparing PGLS or PRMA with Pagel's λ estimated by maximum likelihood, to equivalent models in which Pagel's λ was set to 0. When using Pagel's λ , to assess normality and homoscedasticity assumptions we first extracted phylogenetic residuals. For PGLS, the function 'residuals' was used to extract normalized residuals; for PRMA, a custom code derived from an original provided by R. P. Freckleton was used to produce an equivalent transformation of raw residuals obtained from phyl.RMA. Normality was tested using Anderson Darling tests¹⁵⁴ and heteroscedasticity using Bartlett's test¹³⁰. Additionally, PGLS was used to estimate Pagel's λ for phylogenetic residuals, which should be 0.

The PGLS and PRMA approaches used to test for scaling relationships of vein traits with leaf dimensions and to estimate the slopes of linearized power law relationships are phylogenetic approaches equivalent to ordinary least squares and reduced major axis regressions, respectively. The decision of which of the two to use depended on the specific relationship tested. The least squares approach is preferable in cases when a dependent Y variable is related to an independent X variable, specifically when (1) there is much less error (that is, natural variation and/or measurement error) in X than Y and/or when (2) conceptually, Y is causally determined by or to be predicted from X , but never X from Y ^{155,156}. By contrast, the reduced major axis approach is preferable in cases in which (1) X and Y have similar error and/or in which (2) X or Y are codetermined, or their relationship arises from an underlying functional coordination or either could reasonably be predicted using the other; this approach is typically used in studies of allometric scaling relationships among functional traits or organ dimensions^{155,156}. An exception to the use of reduced major axis for allometry is when testing whether the allometric slope of a relationship is consistent with an expected slope that was derived algebraically from other equations, as only least-squares slopes are robust to algebraic manipulation¹⁵⁶. For example, PGLS would be selected over PRMA to test an expectation for the scaling slope of VSA with leaf length that was derived algebraically by multiplying the expected scaling slopes of VLA and VD with leaf length, given that VSA is determined from VLA and VD (as described in 'Quantification of leaf dimensions and vein traits'). Further, although the least squares approach is appropriate for testing relationships of a dependent versus an independent trait, the reduced major axis approach can be preferable for illustrating the relationship in a plot, as it captures more closely the central trend among two variables with high and/or similar error^{155,156}.

Thus, we selected PGLS or PRMA for the tested relationships according to which was most appropriate given the above principles; the application of any single approach globally would not affect the findings of the study, but would reduce the accuracy of the specific slope estimates. We used PRMA to test relationships of traits with climate variables, as the magnitude of variation in modelled climate variables globally was similar to that for species means for leaf traits. We also used PRMA for testing scaling relationships of vein diameters with leaf length and width, and of xylem conduit diameters with vein diameters, given the preference of this approach for testing allometric relationships, and the similar error in the X and Y variables. We used PGLS for testing relationships of VLA, VSA, VPA and VVA with leaf dimensions, given the higher variability in the vein traits than leaf dimensions arising owing to their determination from one or more vein traits as well as leaf dimensions (for example, VLA = vein number/leaf width). Further, PGLS was most appropriate for testing allometric slopes for the relationships of vein traits to leaf area, because the expectations for these slopes from the

developmental model were derived algebraically from expected slopes of vein traits in relation to leaf length and leaf width¹⁵⁵. Finally, we used PRMA in all figure plots to most clearly illustrate the central trends accounting for phylogeny^{155,156}.

Finally, we evaluated whether the scaling of vein traits with leaf dimensions differed between C₃ and C₄ species. C₃ and C₄ species were considered to differ significantly in trait–trait or trait–climate associations if significant relationships were found independently for both groups, and if there was no overlap in scaling slope 95% confidence intervals using the selected regression approach (PGLS or PRMA).

Modelling the effects of leaf energy budget and testing hypotheses for the benefits of smaller leaves under different climates

We considered three hypotheses for the advantage of small leaf sizes in cold or dry climates on the basis of their thinner boundary layer. Smaller leaves have been hypothesized to (1) experience less damage under extreme temperatures (that is, chilling on cold nights and overheating on hot days)^{3,157,158}, (2) maintain higher rates of photosynthesis and/or higher leaf water-use efficiency in cold and/or dry conditions^{19,20} and (3) achieve higher gas exchange in favourable, warm and wet climates⁴, which would provide an advantage in mitigating the shorter diurnal and/or seasonal growing periods of cold or dry climates.

To test hypothesis (1) (that is, that small grass leaves are typical in cold or dry climates globally because they avoid extreme temperatures), we calculated the minimum threshold of leaf size for chilling or overheating. We used the 100-cm² leaf size threshold for damage by night-time chilling and 30 cm² for damage by daytime overheating (that is, the lowest thresholds that were modelled for eudicotyledons globally, given in figure 3 of ref.³). These leaf size thresholds for eudicotyledons were derived from estimated damage thresholds based on the 'characteristic dimension' of the leaf (d) (that is, the diameter of the largest circle that can be delimited within a leaf) of 8.16 cm and 4.47 cm, according to equation (4) in the supplementary information of ref.³ (LA = 1.5 d^2). Thus, we used these threshold values to exclude species with leaf width >8.16 cm and >4.47 cm, and then tested whether the observed trends of leaf dimensions with MAT and MAP globally remained. Significant trends for this restricted species set would indicate that thresholds for leaf damage under extreme temperatures cannot explain trends for grasses with leaves smaller than those thresholds. By testing trends against these very low thresholds, we provided a very conservative test to establish that avoidance of extreme temperatures would not explain the global climatic distribution of grass leaf size.

To test hypotheses (2) and (3), we used heuristic leaf energy balance modelling to simulate the consequences for gas exchange of leaf sizes varying in size¹⁵⁹. Using the Tealeaves R package¹⁵⁹, given inputs of leaf width, wind speed, stomatal conductance and air temperature, we simulated boundary layer conductance, leaf temperature and transpiration rate. To represent the bulk of the global range of grass leaf size, we focused on comparing the global 5th and 95th quantiles of leaf width (0.1 cm and 2.7 cm). We simulated leaves in wet and dry conditions by setting stomatal conductance values at 0.4 mol m⁻² s⁻¹ and 0.2 mol m⁻² s⁻¹, respectively¹⁶⁰; our tests showed that selecting other values would yield similar qualitative results. To represent warm and cold climates we simulated gas exchange under air temperatures of 315 K and 280 K (41.85 °C and 6.85 °C, respectively)¹⁶¹. All other physical and environmental inputs were maintained constant at typical values¹⁵⁹. We used the output values of leaf temperature and boundary layer conductance to simulate C₃ photosynthetic rate for leaves of different widths using the Farquhar model^{162,163}. We tested these effects at the two wind speeds, 0.1 m s⁻¹ and 2 m s⁻¹. Finally, we tested simulations for both amphistomatic and hypostomatic leaves, and we present results for amphistomatic leaves given that most grasses are amphistomatic¹⁶⁴. To test for the potential benefit of smaller leaves, we calculated the ratios of photosynthetic rate, transpiration and leaf water-use efficiency for

Article

a small relative to large leaf; values >1 indicate an advantage for the small leaf in cold or dry conditions. To test for the potential benefit of smaller leaves in mitigating a shorter period with favourable climate, we calculated the ratios of photosynthetic rate, transpiration and leaf water-use efficiency under warm and wet conditions for a small versus a large leaf; again, values >1 reflect a small leaf advantage.

Reporting summary

Further information on research design is available in the Nature Research Reporting Summary linked to this paper.

Data availability

All data are available in the Article and its Supplementary Information. Leaf trait data for the 1,752 grass species was provided by the published Kew Grassbase Database (<http://www.kew.org/data/grassbase/>). Climate data for species were extracted from WorldClim 2.5-arc minute resolution (<https://www.worldclim.org/>) and from CRU TS4.01 O1 (https://crudata.uea.ac.uk/cru/data/hrg/cru_ts_4.01/) on the basis of the geographical records for each species (<http://www.gbif.org>). Photosynthetic trait data and field locations were extracted for the 13 C₃ grass species for which this was available in GLOPNET (<http://bio.mq.edu.au/~iwright/glopiant.htm>). Source data are provided with this paper.

Code availability

Custom-written R code is available on GitHub (<https://github.com/smuel-taylor/grass-leaf-size->).

48. Kluyver, T. A. & Osborne, C. P. Taxonome: a software package for linking biological species data. *Ecol. Evol.* **3**, 1262–1265 (2013).
49. Cayuela, L., Granzow-de la Cerda, I., Albuquerque, F. S. & Golicher, D. J. TAXONSTAND: an R package for species names standardisation in vegetation databases. *Methods Ecol. Evol.* **3**, 1078–1083 (2012).
50. Fick, S. E. & Hijmans, R. J. WorldClim 2: new 1-km spatial resolution climate surfaces for global land areas. *Int. J. Climatol.* **37**, 4302–4315 (2017).
51. Cherlet, M. H. C., Reynolds, J., Hill, J., Sommer, S. & von Maltitz, G. *World Atlas of Desertification* 3rd edn (Publication Office of the European Union, 2018).
52. Harris, I., Jones, P. D., Osborn, T. J. & Lister, D. H. Updated high-resolution grids of monthly climatic observations – the CRU TS3.10 dataset. *Int. J. Climatol.* **34**, 623–642 (2014).
53. Lasky, J. R. et al. Characterizing genomic variation of *Arabidopsis thaliana*: the roles of geography and climate. *Mol. Ecol.* **21**, 5512–5529 (2012).
54. Sexton, J. P., McIntyre, P. J., Angert, A. L. & Rice, K. J. Evolution and ecology of species range limits. *Annu. Rev. Ecol. Evol. Syst.* **40**, 415–436 (2009).
55. Dengler, N. G., Dengler, R. E. & Hattersley, P. W. Differing ontogenetic origins of PCR (Kranz) sheaths in leaf blades of C₄ grasses (Poaceae). *Am. J. Bot.* **72**, 284–302 (1985).
56. Dengler, N. G., Woodvine, M. A., Donnelly, P. M. & Dengler, R. E. Formation of vascular pattern in developing leaves of the C₄ grass *Arundinella hirta*. *Int. J. Plant Sci.* **158**, 1–12 (1997).
57. Ikenberry, G.-J. *Developmental Vegetative Morphology of Avena sativa*. PhD thesis, Iowa State Univ. (1959).
58. Kaufman, P. B. & Brock, T. G. in *Oat Science and Technology* (eds Marshall, H. G. & Sorrells, M. E.) 53–75 (American Society of Agronomy, 1992).
59. Hitch, P. A. & Sharman, B. C. Initiation of procambial strands in leaf primordia of *Dactylis glomerata* L as an example of a temperate herbage grass. *Ann. Bot.* **32**, 153–164 (1968).
60. Davidson, J. L. & Milthorpe, F. L. Leaf growth in *Dactylis glomerata* following defoliation. *Ann. Bot.* **30**, 173–184 (1966).
61. Volenec, J. J. & Nelson, C. J. Cell dynamics in leaf meristems of contrasting tall fescue genotypes. *Crop Sci.* **21**, 381–385 (1981).
62. Macadam, J. W. & Nelson, C. J. Specific leaf weight in zones of cell division, elongation and maturation in tall fescue leaf blades. *Ann. Bot.* **59**, 369–376 (1987).
63. MacAdam, J. W., Volenec, J. J. & Nelson, C. J. Effects of nitrogen on mesophyll cell division and epidermal cell elongation in tall fescue leaf blades. *Plant Physiol.* **89**, 549–556 (1989).
64. Skinner, R. H. & Nelson, C. J. Elongation of the grass leaf and its relationship to the phyllochron. *Crop Sci.* **35**, 4–10 (1995).
65. Skinner, R. H. & Nelson, C. J. Epidermal cell division and the coordination of leaf and tiller development. *Ann. Bot.* **74**, 9–15 (1994).
66. Maurice, I., Gastal, F. & Durand, J. L. Generation of form and associated mass deposition during leaf development in grasses: a kinematic approach for non-steady growth. *Ann. Bot.* **80**, 673–683 (1997).
67. Durand, J. L., Schaufele, R. & Gastal, F. Grass leaf elongation rate as a function of developmental stage and temperature: morphological analysis and modelling. *Ann. Bot.* **83**, 577–588 (1999).
68. Martre, P., Durand, J. L. & Cochard, H. Changes in axial hydraulic conductivity along elongating leaf blades in relation to xylem maturation in tall fescue. *New Phytol.* **146**, 235–247 (2000).
69. Martre, P. & Durand, J. L. Quantitative analysis of vasculature in the leaves of *Festuca arundinacea* (Poaceae): Implications for axial water transport. *Int. J. Plant Sci.* **162**, 755–766 (2001).
70. Gallagher, J. N. Field studies of cereal leaf growth 1. Initiation and expansion in relation to temperature and ontogeny. *J. Exp. Bot.* **30**, 625–636 (1979).
71. Gallagher, J. N. & Biscoe, P. V. Field studies of cereal leaf growth 3. Barley leaf extension in relation to temperature, irradiance, and water potential. *J. Exp. Bot.* **30**, 645–655 (1979).
72. Dannenhoffer, J. M., Ebert, W. & Evert, R. F. Leaf vasculature in barley, *Hordeum vulgare* (Poaceae). *Am. J. Bot.* **77**, 636–652 (1990).
73. Dannenhoffer, J. M. & Evert, R. F. Development of the vascular system in the leaf of barley (*Hordeum vulgare* L.). *Int. J. Plant Sci.* **155**, 143–157 (1994).
74. Trivett, C. L. & Evert, R. F. Ontogeny of the vascular bundles and contiguous tissues in the barley leaf blade. *Int. J. Plant Sci.* **159**, 716–723 (1998).
75. Soper, K. & Mitchell, K. J. The developmental anatomy of perennial ryegrass (*Lolium perenne* L.). *N. Z. J. Sci. Technol.* **37**, 484–504 (1956).
76. Schnyder, H., Nelson, C. J. & Coutts, J. H. Assessment of spatial distribution of growth in the elongation zone of grass leaf blades. *Plant Physiol.* **85**, 290–293 (1987).
77. Arredondo, J. T. & Schnyder, H. Components of leaf elongation rate and their relationship to specific leaf area in contrasting grasses. *New Phytol.* **158**, 305–314 (2003).
78. Kauffman, P. B. Development of the shoot of *Oryza sativa* L. – II. Leaf histogenesis. *Phytomorphology* **9**, 277–311 (1959).
79. Yamazaki, K. Studies on the leaf formation in rice plants: I. Observation on the successive development of the leaf. *Jpn. J. Crop. Sci.* **31**, 371–378 (1963).
80. Chonan, N. K. H. & Matsuda, T. Morphology on vascular bundles of leaves in gramineous crops: I. Observations on vascular bundles of leaf blades, sheaths and internodes in riceplants. *Jpn. J. Crop. Sci.* **43**, 425–432 (1974).
81. Hoshikawa, K. *The Growing Rice Plant: An Anatomical Monograph* (Nobunkyo, 1989).
82. Matsukura, C. et al. Transverse vein differentiation associated with gas space formation – fate of the middle cell layer in leaf sheath development of rice. *Ann. Bot.* **85**, 19–27 (2000).
83. Itoh, J. et al. Rice plant development: from zygote to spikelet. *Plant Cell Physiol.* **46**, 23–47 (2005).
84. Sakaguchi, J. & Fukuda, H. Cell differentiation in the longitudinal veins and formation of commissural veins in rice (*Oryza sativa*) and maize (*Zea mays*). *J. Plant Res.* **121**, 593–602 (2008).
85. Parent, B., Conejero, G. & Tardieu, F. Spatial and temporal analysis of non-steady elongation of rice leaves. *Plant Cell Environ.* **32**, 1561–1572 (2009).
86. Begg, J. E. & Wright, M. J. Growth and development of leaves from intercalary meristems in *Phalaris arundinacea* L. *Nature* **194**, 1097–1098 (1962).
87. Colbert, J. T. & Evert, R. F. Leaf vasculature in sugarcane (*Saccharum officinarum* L.). *Planta* **156**, 136–151 (1982).
88. Bernstein, N., Silk, W. K. & Lauchli, A. Growth and development of sorghum leaves under conditions of NaCl stress – spatial and temporal aspects of leaf growth inhibition. *Planta* **191**, 433–439 (1993).
89. Sud, R. M. & Dengler, N. G. Cell lineage of vein formation in variegated leaves of the C₄ grass *Stenotaphrum secundatum*. *Ann. Bot.* **86**, 99–112 (2000).
90. Sharman, B. C. & Hitch, P. A. Initiation of procambial strands in leaf primordia of bread wheat *Triticum aestivum* L. *Ann. Bot.* **31**, 229–243 (1967).
91. Blackman, E. The morphology and development of cross veins in the leaves of bread wheat (*Triticum aestivum* L.). *Ann. Bot.* **35**, 653–665 (1971).
92. Kemp, D. R. The location and size of the extension zone of emerging wheat leaves. *New Phytol.* **84**, 729–737 (1980).
93. Paolillo, D. J. Protoxylem maturation in the seedling leaf of wheat. *Am. J. Bot.* **82**, 337–345 (1995).
94. Beemster, G. T. S. & Masle, J. The role of apical development around the time of leaf initiation in determining leaf width at maturity in wheat seedlings (*Triticum aestivum* L.) with impeded roots. *J. Exp. Bot.* **47**, 1679–1688 (1996).
95. Sharman, B. C. Developmental anatomy of the shoot of *Zea mays* L. *Ann. Bot.* **6**, 245–282 (1942).
96. Esau, K. Ontogeny of the vascular bundle in *Zea mays*. *Hilgardia* **15**, 325–368 (1943).
97. Bosabalidis, A. M., Evert, R. F. & Russin, W. A. Ontogeny of the vascular bundles and contiguous tissues in the maize leaf blade. *Am. J. Bot.* **81**, 745–752 (1994).
98. Poethig, S. in *Contemporary Problems in Plant Anatomy* (eds Dickison R. A. & White, W. C.) 235–259 (Academic, 1984).
99. Russell, S. H. & Evert, R. F. Leaf vasculature in *Zea mays* L. *Planta* **164**, 448–458 (1985).
100. Smith, L. G., Greene, B., Veit, B. & Hake, S. A dominant mutation in the maize homeobox gene, Knotted-1, causes its ectopic expression in leaf cells with altered fates. *Development* **116**, 21–30 (1992).
101. Fournier, C. & Andrieu, B. A 3D architectural and process-based model of maize development. *Ann. Bot.* **81**, 233–250 (1998).
102. Muller, B., Reymond, M. & Tardieu, F. The elongation rate at the base of a maize leaf shows an invariant pattern during both the steady-state elongation and the establishment of the elongation zone. *J. Exp. Bot.* **52**, 1259–1268 (2001).
103. Muller, B. et al. Association of specific expansins with growth in maize leaves is maintained under environmental, genetic, and developmental sources of variation. *Plant Physiol.* **143**, 278–290 (2007).
104. Johnston, R., Leiboff, S. & Scanlon, M. J. Ontogeny of the sheathing leaf base in maize (*Zea mays*). *New Phytol.* **205**, 306–315 (2015).
105. Ben-Haj-Salah, H. & Tardieu, F. Temperature affects expansion rate of maize leaves without change in spatial distribution of cell length – analysis of the coordination between cell division and cell expansion. *Plant Physiol.* **109**, 861–870 (1995).
106. Tardieu, F., Reymond, M., Hamard, P., Granier, C. & Muller, B. Spatial distributions of expansion rate, cell division rate and cell size in maize leaves: a synthesis of the effects of soil water status, evaporative demand and temperature. *J. Exp. Bot.* **51**, 1505–1514 (2000).
107. Runions, A. et al. Modeling and visualization of leaf venation patterns. *ACM Trans. Graphic.* **24**, 702–711 (2005).

108. Scarpella, E. & Meijer, A. H. Pattern formation in the vascular system of monocot and dicot plant species. *New Phytol.* **164**, 209–242 (2004).
109. Baskin, T. I. Anisotropic expansion of the plant cell wall. *Annu. Rev. Cell. Dev.* **21**, 203–222 (2005).
110. Fujita, H. & Mochizuki, A. The origin of the diversity of leaf venation pattern. *Dev. Dyn.* **235**, 2710–2721 (2006).
111. Granier, C. & Tardieu, F. Multi-scale phenotyping of leaf expansion in response to environmental changes: the whole is more than the sum of parts. *Plant Cell Environ.* **32**, 1175–1184 (2009).
112. Scarpella, E., Barkoulas, M. & Tsiantis, M. Control of leaf and vein development by auxin. *Cold Spring Harb. Perspect. Biol.* **2**, a001511 (2010).
113. Gámez, A. & Beemster, G. T. S. What determines organ size differences between species? A meta-analysis of the cellular basis. *New Phytol.* **215**, 299–308 (2017).
114. Scarpella, E. The logic of plant vascular patterning. Polarity, continuity and plasticity in the formation of the veins and of their networks. *Curr. Opin. Genet. Dev.* **45**, 34–43 (2017).
115. Berlyn, G. P. M. J. P. *Botanical Microtechnique and Cytochemistry* (Iowa State Univ. Press, 1976).
116. Kemp, C. D. Methods of estimating leaf area of grasses from linear measurements. *Ann. Bot.* **24**, 491–499 (1960).
117. Stickler, F. C., Wearden, S. & Pauli, A. W. Leaf area determination in grain sorghum. *Agronomy* **53**, 187–188 (1961).
118. Shi, P. et al. Leaf-area-length allometry and its implications in leaf shape evolution. *Trees* **33**, 1073–1085 (2019).
119. Ellis, R. P. A procedure for standardizing comparative leaf anatomy in the Poaceae. I. The leaf blade as viewed in transverse section. *Bothalia* **12**, 65–109 (1976).
120. Evert, R. F. *Esau's Plant Anatomy: Meristems, Cells, and Tissues of the Plant Body: Their Structure, Function, and Development* (John Wiley, 2006).
121. Neufeld, H. S. et al. Genotypic variability in vulnerability of leaf xylem to cavitation in water-stressed and well-irrigated sugarcane. *Plant Physiol.* **100**, 1020–1028 (1992).
122. Tyree, M. T., Zimmermann, M. H. & Zimmermann, M. H. *Xylem Structure and the Ascent of Sap* 2nd edn (Springer, 2002).
123. Wright, I. J. et al. The worldwide leaf economics spectrum. *Nature* **428**, 821–827 (2004).
124. Grass Phylogeny Working Group II. New grass phylogeny resolves deep evolutionary relationships and discovers *C₄* origins. *New Phytol.* **193**, 304–312 (2012).
125. Taylor, S. H. et al. Photosynthetic pathway and ecological adaptation explain stomatal trait diversity amongst grasses. *New Phytol.* **193**, 387–396 (2012).
126. Edgar, R. C. MUSCLE: multiple sequence alignment with high accuracy and high throughput. *Nucleic Acids Res.* **32**, 1792–1797 (2004).
127. Drummond, A. J. & Rambaut, A. BEAST: Bayesian evolutionary analysis by sampling trees. *BMC Evol. Biol.* **7**, 214 (2007).
128. Christin, P. A. et al. Molecular dating, evolutionary rates, and the age of the grasses. *Syst. Biol.* **63**, 153–165 (2014).
129. Prasad, V. et al. Late Cretaceous origin of the rice tribe provides evidence for early diversification in Poaceae. *Nat. Commun.* **2**, 480 (2011).
130. R Core Team. *R: A Language and Environment for Statistical Computing*, <http://www.R-project.org/> (R Foundation for Statistical Computing, 2019).
131. Paradis, E. & Schliep, K. ape 5.0: an environment for modern phylogenetics and evolutionary analyses in R. *Bioinformatics* **35**, 526–528 (2019).
132. Spriggs, E. L., Christin, P.-A. & Edwards, E. J. Data from: *C₄* photosynthesis promoted species diversification during the Miocene grassland expansion, <https://doi.org/10.5061/dryad.74b5d> (2015).
133. Felsenstein, J. Phylogenies and the comparative method. *Am. Nat.* **125**, 1–15 (1985).
134. Schmerler, S. B. et al. Evolution of leaf form correlates with tropical–temperate transitions in *Viburnum* (Adoxaceae). *Proc. R. Soc. B.* **279**, 3905–3913 (2012).
135. Fletcher, L. R. et al. Evolution of leaf structure and drought tolerance in species of Californian *Ceanothus*. *Am. J. Bot.* **105**, 1672–1687 (2018).
136. Bramer, I. et al. in *Next Generation Biomonitoring: Part 1 (Advances in Ecological Research, volume 58)* (eds. Bohan, D. A. et al.) 101–161 (Academic, 2018).
137. Zanne, A. E. et al. Three keys to the radiation of angiosperms into freezing environments. *Nature* **506**, 89–92 (2014).
138. Watcharamongkol, T., Christin, P. A. & Osborne, C. P. C. *C₄* photosynthesis evolved in warm climates but promoted migration to cooler ones. *Ecol. Lett.* **21**, 376–383 (2018).
139. Burnham, K. P. & Anderson, D. R. *Model Selection and Multimodel Inference* 2nd edn (Springer, 2002).
140. Gelman, A. & Hill, J. *Data Analysis Using Regression and Multilevel/Hierarchical Models* (Cambridge Univ. Press, 2006).
141. Faraway, J. J. *Linear Models with R* (Chapman & Hall, 2009).
142. Murray, K. & Conner, M. M. Methods to quantify variable importance: implications for the analysis of noisy ecological data. *Ecology* **90**, 348–355 (2009).
143. Westoby, M. & Wright, I. J. Land-plant ecology on the basis of functional traits. *Trends Ecol. Evol.* **21**, 261–268 (2006).
144. Grubb, P. J. Trade-offs in interspecific comparisons in plant ecology and how plants overcome proposed constraints. *Plant Ecol. Divers.* **9**, 3–33 (2016).
145. Cade, B. S. & Noon, B. R. A gentle introduction to quantile regression for ecologists. *Front. Ecol. Environ.* **1**, 412–420 (2003).
146. Grubb, P. J., Coomes, D. A. & Metcalfe, D. J. Comment on “A brief history of seed size”. *Science* **310**, 783 (2005).
147. Moles, A. T. et al. Global patterns in plant height. *J. Ecol.* **97**, 923–932 (2009).
148. Pagel, M. Inferring the historical patterns of biological evolution. *Nature* **401**, 877–884 (1999).
149. Freckleton, R. P., Harvey, P. H. & Pagel, M. Phylogenetic analysis and comparative data: a test and review of evidence. *Am. Nat.* **160**, 712–726 (2002).
150. Pinheiro, J. et al. nlme: linear and nonlinear mixed effect models. R package version 3.1-140, <https://CRAN.R-project.org/package=nlme> (2019).
151. Revell, L. J. phytos: an R package for phylogenetic comparative biology (and other things). *Methods Ecol. Evol.* **3**, 217–223 (2012).
152. Warton, D. I., Wright, I. J., Falster, D. S. & Westoby, M. Bivariate line-fitting methods for allometry. *Biol. Rev. Camb. Philos. Soc.* **81**, 259–291 (2006).
153. Garland, T., Dickerman, A. W., Janis, C. M. & Jones, J. A. Phylogenetic analysis of covariance by computer-simulation. *Syst. Biol.* **42**, 265–292 (1993).
154. Gross, J. & Ligges, U. nortest: tests for normality. R package version 1.0-4, <https://cran.r-project.org/package=nortest> (2015).
155. Poorter, H. & Sack, L. Pitfalls and possibilities in the analysis of biomass allocation patterns in plants. *Front. Plant Sci.* **3**, 259 (2012).
156. Smith, R. J. Use and misuse of the reduced major axis for line-fitting. *Am. J. Phys. Anthropol.* **140**, 476–486 (2009).
157. Gates, D. M. Energy, plants, and ecology. *Ecology* **46**, 1–13 (1965).
158. Lusk, C. H. et al. Frost and leaf-size gradients in forests: global patterns and experimental evidence. *New Phytol.* **219**, 565–573 (2018).
159. Muir, C. D. tealeaves: an R package for modelling leaf temperature using energy budgets. *AoB Plants* **11**, plz054 (2019).
160. Taylor, S. H. et al. Ecophysiological traits in *C₃* and *C₄* grasses: a phylogenetically controlled screening experiment. *New Phytol.* **185**, 780–791 (2010).
161. Huang, M. et al. Air temperature optima of vegetation productivity across global biomes. *Nat. Ecol. Evol.* **3**, 772–779 (2019).
162. Farquhar, G. D., von Caemmerer, S. & Berry, J. A. A biochemical model of photosynthetic CO₂ assimilation in leaves of *C₃* species. *Planta* **149**, 78–90 (1980).
163. Bernacchi, C. J., Pimentel, C. & Long, S. P. In vivo temperature response functions of parameters required to model RuBP-limited photosynthesis. *Plant Cell Environ.* **26**, 1419–1430 (2003).
164. Muir, C. D. Making pore choices: repeated regime shifts in stomatal ratio. *Proc. R. Soc. B.* **282**, 1–9 (2012).
165. Brummitt, R. K. *World Geographical Scheme for Recording Plant Distributions* (Hunt Institute for Botanical Documentation, 2001).

Acknowledgements We thank T. Cheng, W. Deng, A. C. Diener, A. Kooner, M. McMaster, C. Muir, S. Moshrefi, A. J. Patel, A. Sayari and M. S. Vorontsova for logistical assistance. Funding was provided by the US National Science Foundation (grants 1457279, 1951244 and 2017949), the Natural Environment Research Council (grants NE/D013062/1 and NE/T000759/1) and a Royal Society University Research Fellowship (grant URF/R180022).

Author contributions The project was conceptualized by A.S.B., S.H.T., C.P.O. and L.S. A.S.B., S.H.T., J.P.-K., C.V., Y.Z., T.W., C.S., E.J.E., P.-A.C., C.P.O. and L.S. performed data curation, and reviewed and edited the manuscript. A.S.B., S.H.T., J.P.-K., C.V., Y.Z., T.W., C.S., P.-A.C. and L.S. undertook formal analyses. C.P.O. and L.S. acquired funding. A.S.B., S.H.T., J.P.-K., T.W., C.S., E.J.E., P.-A.C., C.P.O. and L.S. performed the investigations. A.S.B., S.H.T., J.P.-K., T.W., C.S., E.J.E., P.-A.C., C.P.O. and L.S. developed the methodology. A.S.B., S.H.T., J.P.-K., C.P.O. and L.S. administered the project. A.S.B., S.H.T., J.P.-K., T.W., C.S., E.J.E., P.-A.C., C.P.O. and L.S. provided resources. A.S.B., S.H.T., T.W. and P.-A.C. wrote the software. A.S.B., S.H.T., J.P.-K., C.P.O. and L.S. supervised the project. A.S.B., S.H.T., C.P.O. and L.S. validated the data. A.S.B., S.H.T., T.W., C.S., E.J.E., P.-A.C., C.P.O. and L.S. provided the data visualization. A.S.B., S.H.T. and L.S. wrote the original draft.

Competing interests The authors declare no competing interests.

Additional information

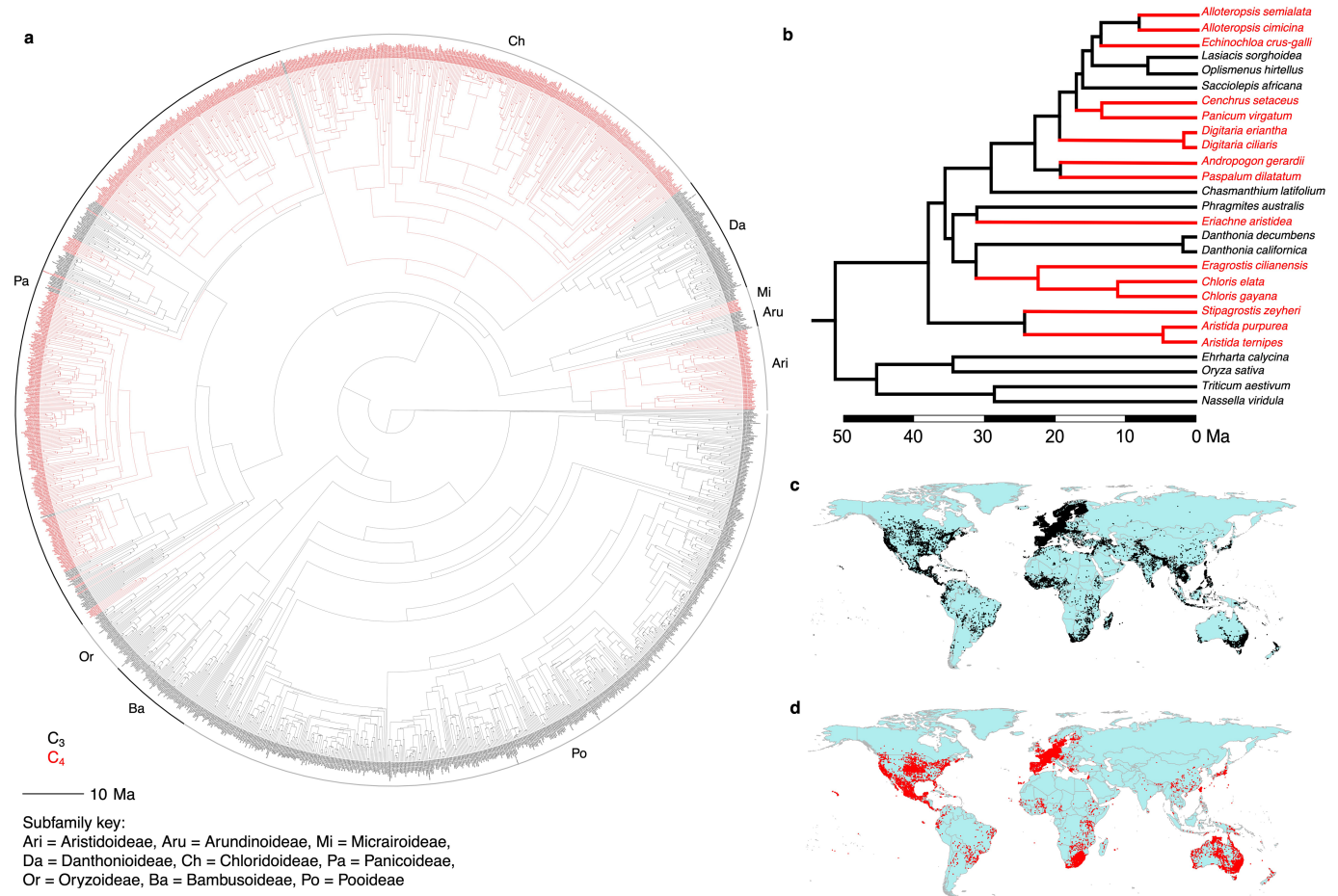
Supplementary information The online version contains supplementary material available at <https://doi.org/10.1038/s41586-021-03370-0>.

Correspondence and requests for materials should be addressed to A.S.B. or L.S.

Peer review information *Nature* thanks Timothy Brodrribb, Ian Wright and the other, anonymous, reviewer(s) for their contribution to the peer review of this work.

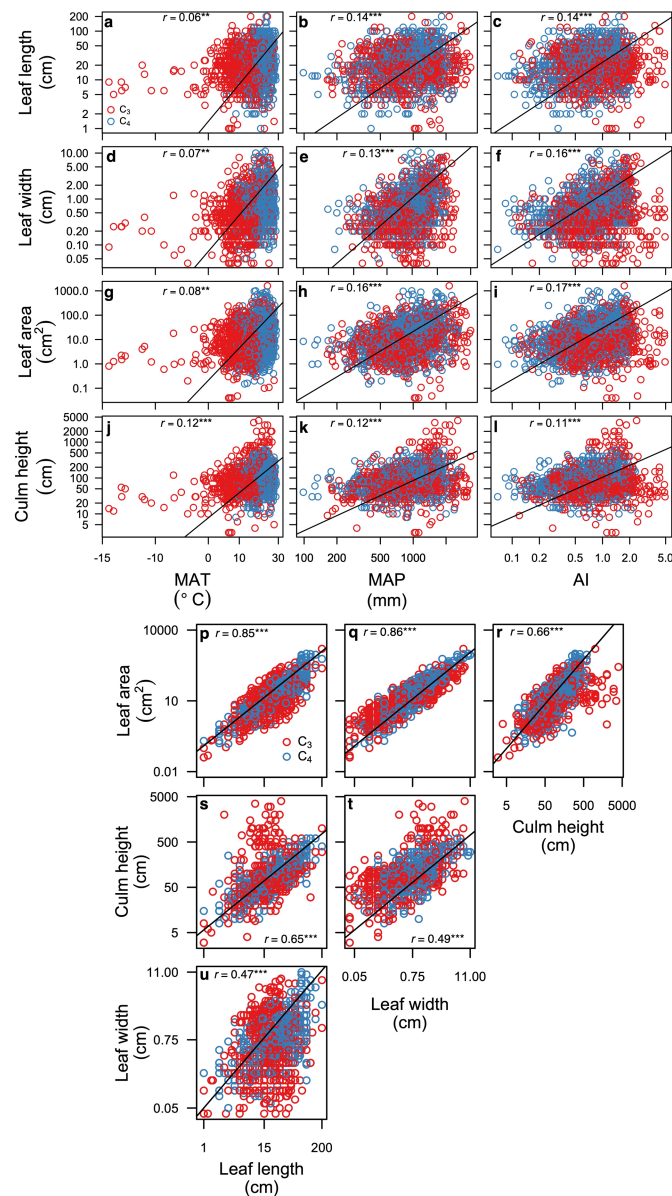
Reprints and permissions information is available at <http://www.nature.com/reprints>.

Article



Extended Data Fig. 1 | Time-calibrated phylogenetic trees for 1,752 worldwide grass species and for 27 grass species grown in a greenhouse common garden. **a**, Phylogeny for 1,752 species, trimmed from a previous publication¹³², used for analyses of global scaling of leaf size with climate. C_3 and C_4 species are in black and red, respectively ($n=840$ and $n=912$,

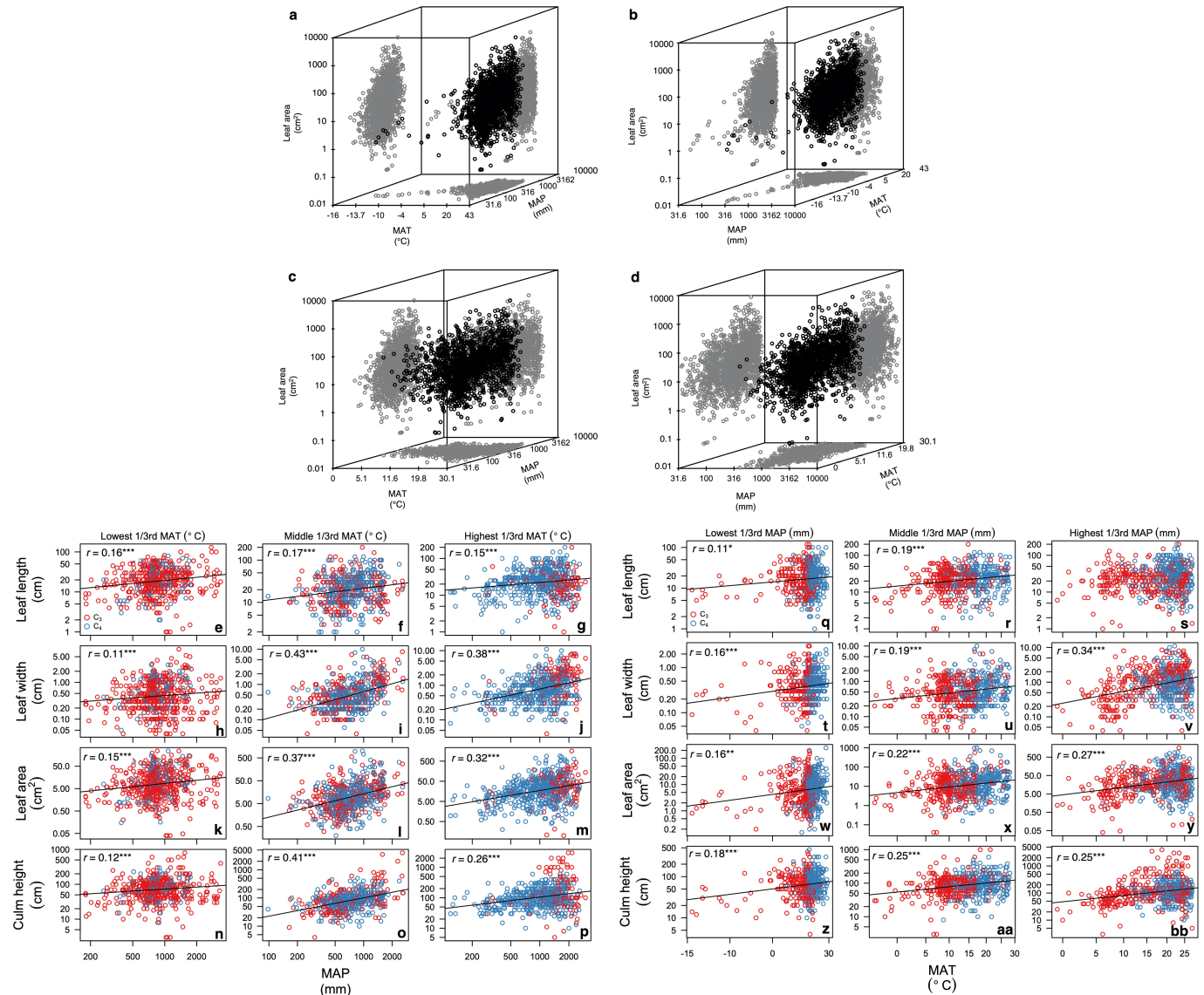
respectively). **b**, Phylogeny for 27 species used for analyses of leaf vein scaling (black branches, 11 C_3 grasses; red branches, 16 C_4 grasses), emphasizing the inclusion of 11 independent C_4 origins. **c, d**, Map of the distributions of the 11 C_3 species (**c**) and 16 C_4 species (**d**).



Extended Data Fig. 2 | Worldwide relationships of grass leaf and plant dimensions with the native climate of species, the global distribution of grass leaf size, and the scaling of grass leaf and plant dimensions.

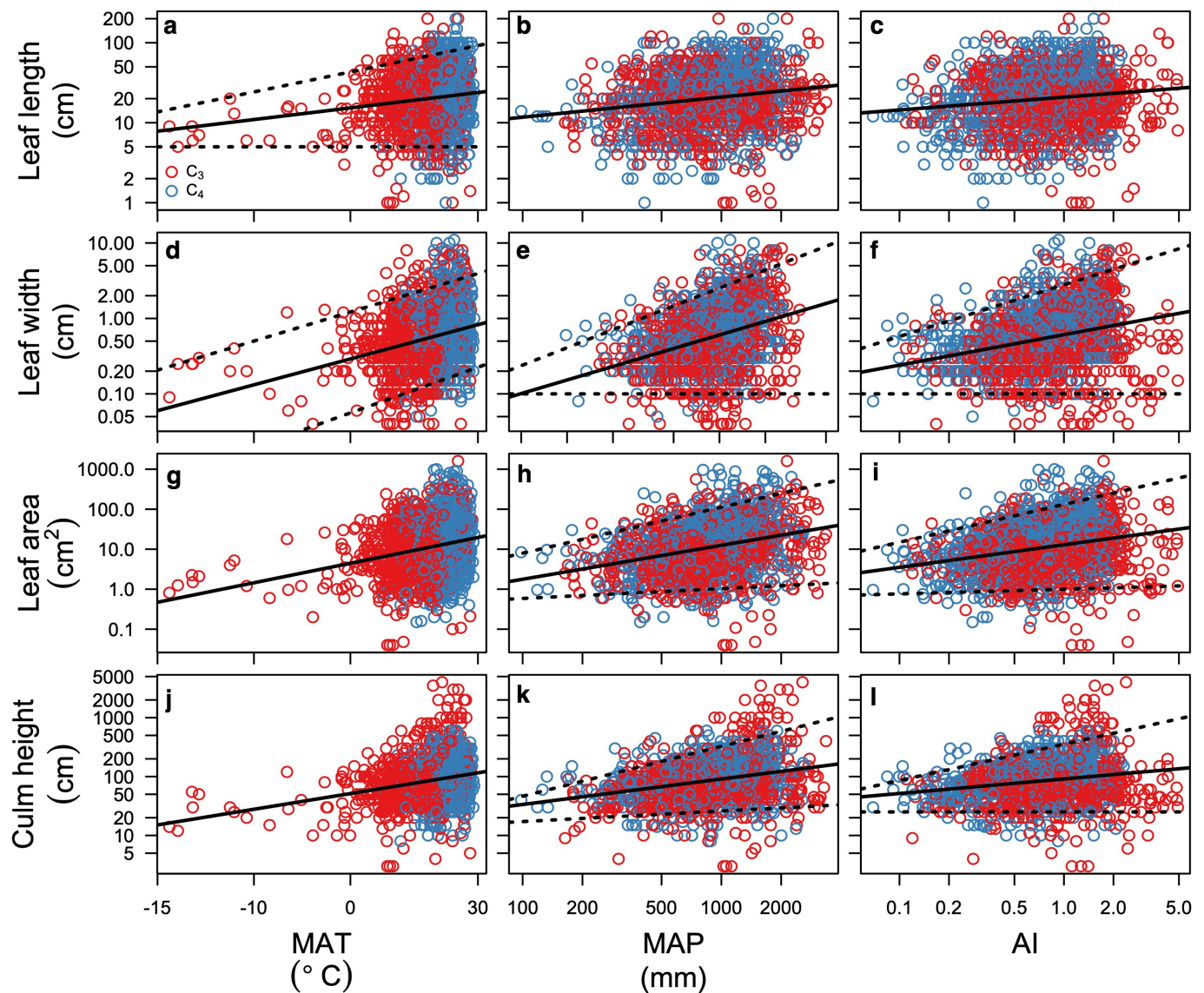
a–l, Relationship of leaf length (**a–c**), leaf width (**d–f**), leaf area (leaf width \times leaf length) (**g–i**) and culm height (**j–l**) with MAT, MAP and the aridity index (AI). **m–o**, Average across species of leaf area for each country in the global database (International Working Group on Taxonomic Databases for Plant Sciences, TDWG level-3 spatial units¹⁶⁵), including countries for which >20 species occur in the global database (21–547 species for each country; grey for countries with <20 species represented); that is, mean leaf area (**m**), median leaf area (**n**) and leaf area for the largest leafed species (**o**). **p–u**, The scaling of leaf area with leaf length (**p**) and leaf width (**q**), leaf area with culm height (**r**), culm height with leaf

length (**s**) and leaf width (**t**), and leaf width with leaf length (**u**). Leaf trait and climate data are provided in Supplementary Table 2. $n=1,752$ globally distributed grass species in **a–i**, **p**, **q**, **u**, and $1,729$ in **j–l**, **r**–**t**. Corresponding regression coefficients for ahistorical analyses of relationships in **a–l**: 0.14, 0.17, 0.14, 0.26, 0.34, 0.28, 0.24, 0.24, 0.31, 0.26, 0.24, 0.29 and 0.3. Two-tailed PRMA regressions were fitted for $\log(\text{trait}) = \log(a) + b \log(\text{trait})$ in **a–l**, **p**–**u**. *** $P < 0.001$, ** $P < 0.01$. $P = 0.0099$ (**a**), 7.8×10^{-9} (**b**), 4.2×10^{-9} (**c**), 0.004 (**d**), 1.8×10^{-8} (**e**), 2.4×10^{-11} (**f**), 0.0014 (**g**), 2.9×10^{-11} (**h**), 2.2×10^{-13} (**i**), 1.7×10^{-6} (**j**), 4.0×10^{-7} (**k**), 1.1×10^{-5} (**l**), about 0 (**p**), about 0 (**q**), 3.17×10^{-219} (**r**), 1.92×10^{-205} (**s**), 7.92×10^{-106} (**t**), 2.7×10^{-96} (**u**). C_3 and C_4 species are shown in red and blue, respectively.



Extended Data Fig. 3 | Worldwide association of grass leaf size with the native climate of the species in 3D, and binned by 1/3rd lowest, middle and highest MAT or MAP in 2D. **a–d**, Leaf area versus climate variables (that is, $x = \text{MAT}$ and $y = \text{MAP}$) (**a, c**); horizontal axes are flipped (that is, leaf area versus $x = \text{MAP}$ and $y = \text{MAT}$) in **b, d**. **e–p**, Relationship of leaf length (**e–g**), leaf width (**h–j**), leaf area (**k–m**) and culm height (**n–p**) to MAP. $n = 584$ globally distributed grass species in **e–m**, and 576 in **n–p**. **q–z, aa, bb**, Relationships of leaf length (**q–s**), leaf width (**t–v**), leaf area (**w–y**) and culm height (**z, aa, bb**) with MAT. $n = 584$ globally distributed grass species in **e–m**, **q–y**, and 576 for **n–p, z, aa, bb**. **In a, b**, data for all species in the global database ($n = 1,752$) are presented; in

c, d, 29 species with MAT $< 0^\circ\text{C}$ are excluded, for a clearer view of the bulk of the species. Projected grey shadows in **a–d** represent the bivariate relationships. Parameters from multiple regression analysis are presented in Supplementary Table 8. Two-tailed ordinary least square regressions were fitted for $\log(\text{trait}) = \log(a) + b \log(\text{climate variable})$ in **e–z, aa, bb**. *** $P < 0.001$, ** $P < 0.01$. $P = 8.1 \times 10^{-5}$ (**e**), 2.2×10^{-5} (**f**), 0.0002 (**g**), 0.0094 (**h**), 8.4×10^{-28} (**i**), 1.7×10^{-18} (**j**), 0.0002 (**k**), 1.1×10^{-20} (**l**), 1.8×10^{-15} (**m**), 0.0028 (**n**), 4.7×10^{-22} (**o**), 2.2×10^{-10} (**p**), 0.0106 (**q**), 2.9×10^{-6} (**r**), 7.0×10^{-5} (**t**), 6.7×10^{-6} (**u**), 1.5×10^{-17} (**v**), 0.0001 (**w**), 7.9×10^{-8} (**x**), 2.6×10^{-11} (**y**), 1.3×10^{-5} (**z**), 1.7×10^{-9} (**aa**), 8.5×10^{-10} (**bb**). C₃ and C₄ species are shown in red and blue, respectively.

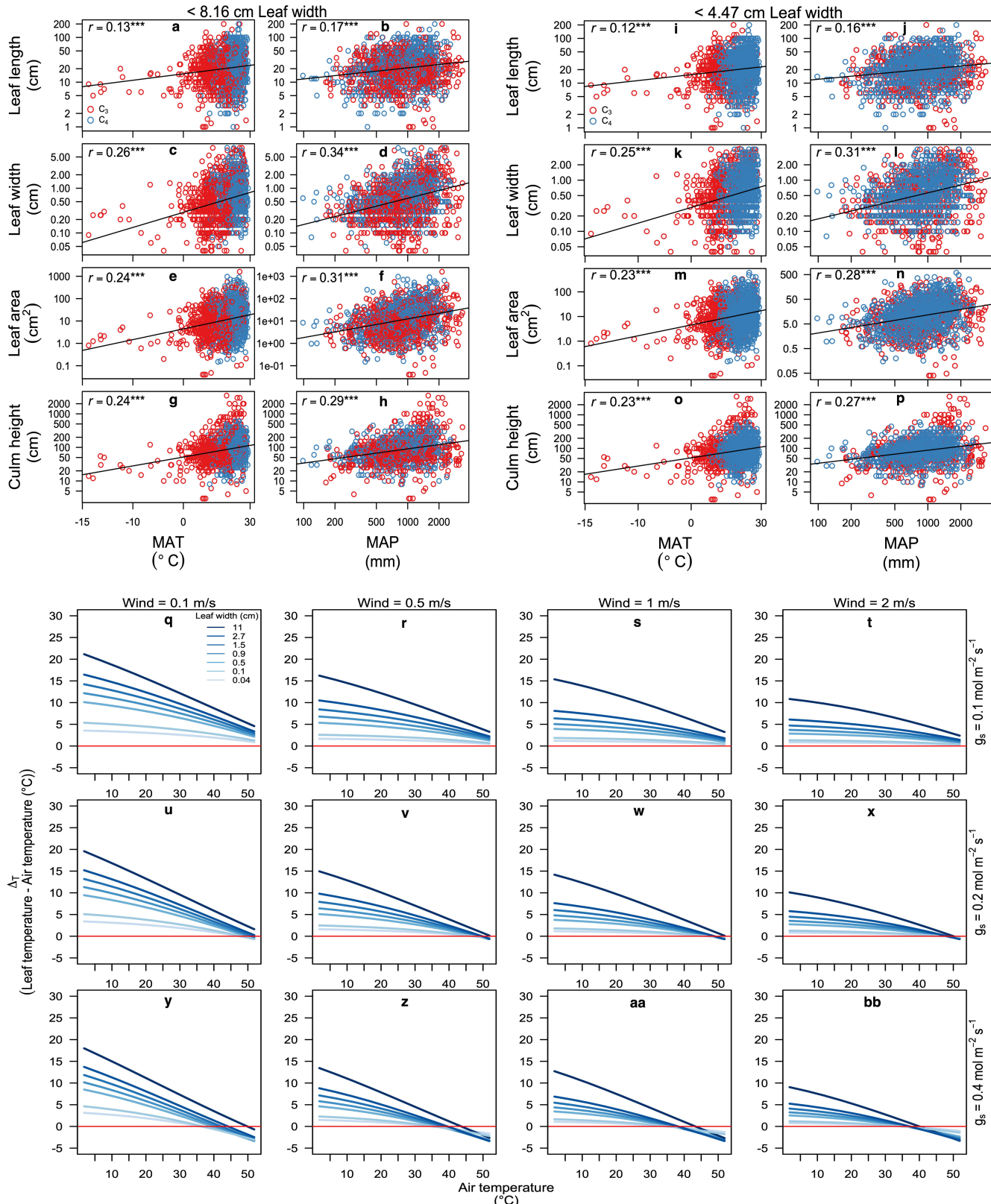


Extended Data Fig. 4 | Quantile regression analyses of worldwide associations of grass leaf traits with the native climate of species.

a–l, Relationship of leaf length (**a–c**), leaf width (**d–f**), leaf area (**g–i**) and culm height (**j–l**) with MAT, MAP and the aridity index. $n=1,752$ globally distributed grass species in **a–i**, and $n=1,729$ in **j–l**. Two-tailed ordinary least square

(solid lines) and 95% and 5% quantile regressions (dotted lines) were fitted for $\log(\text{trait}) = \log(a) + b \log(\text{climate variable})$; quantile lines are drawn if significantly different in slope at $P < 0.05$. C₃ and C₄ species are in red and blue, respectively.

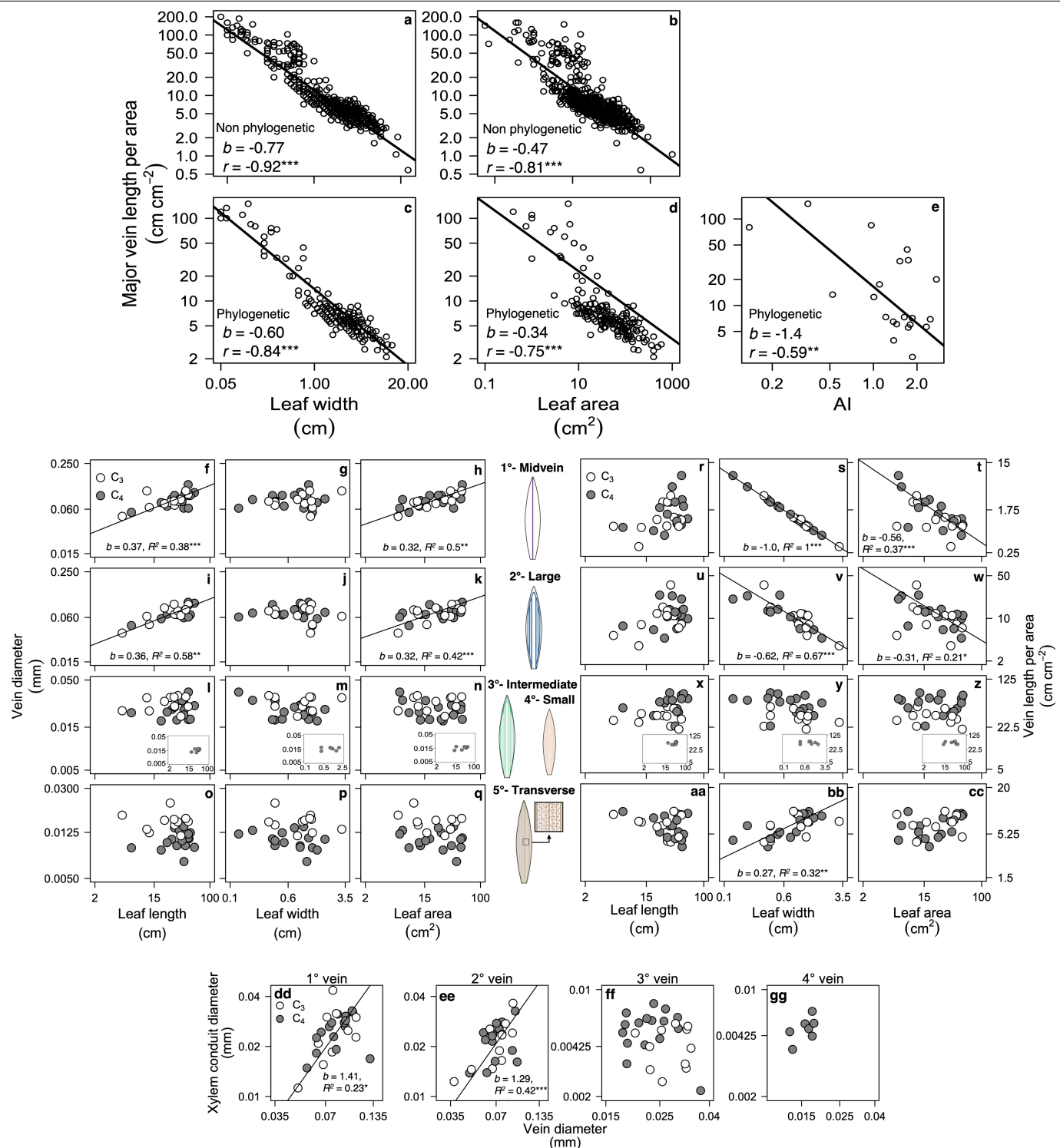
Article



Extended Data Fig. 5 | See next page for caption.

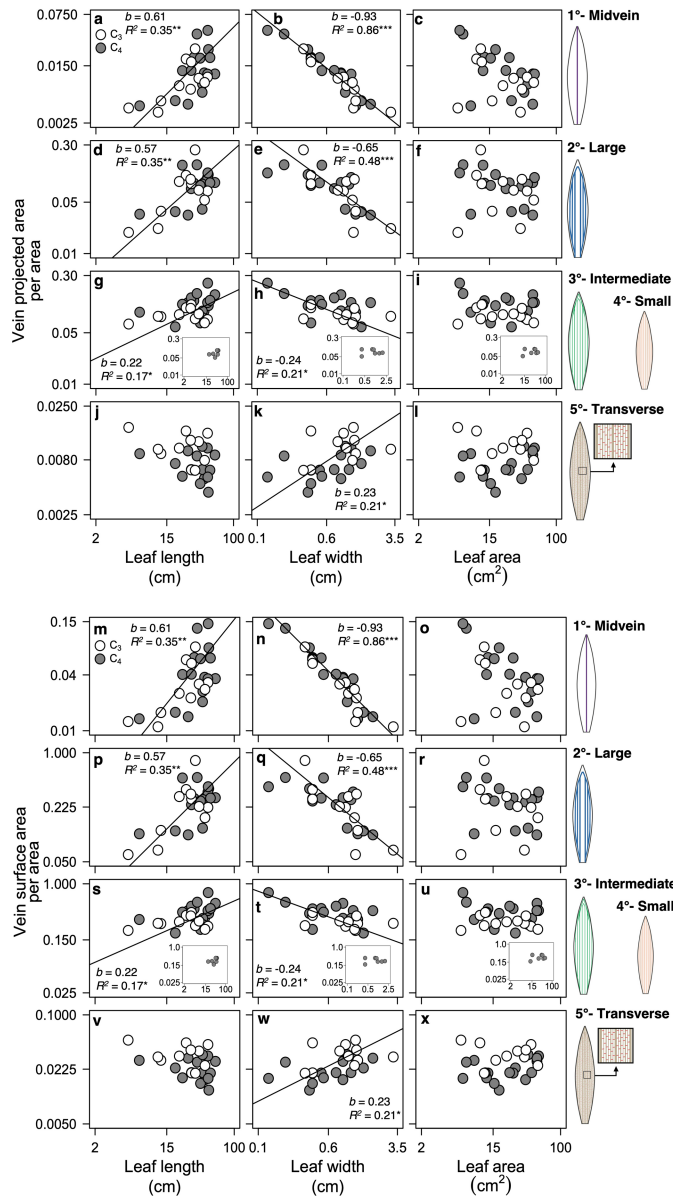
Extended Data Fig. 5 | Worldwide associations of grass leaf and plant dimensions with the native climate of species for species with leaf width <8.16 cm or <4.47 cm (below the modelled threshold for damage owing to night-time chilling or overheating) and modelled leaf temperature difference from air temperature for amiphistomatic grass leaves under different air temperatures. **a–h**, Relationship of leaf length (**a**, **b**), leaf width (**c**, **d**), leaf area (**e**, **f**) and culm height (**g**, **h**) to MAT and MAP for species with leaf width <8.16 cm. **i–p**, Relationships of leaf length (**i**, **j**), leaf width (**k**, **l**), leaf area (**m**, **n**) and culm height (**o**, **p**) to MAT and MAP for species with leaf width <4.47 cm. $n = 1,748$ globally distributed grass species for **a–f**, 1,725 for **g**, **h**, 1,716 for **i–n** and 1,694 for **o**, **p**. **q–z**, **aa**, **bb**, Simulations were run with stomatal

conductance ($\text{mol m}^{-2} \text{s}^{-1}$) 0.1 (**q–t**), 0.2 (**u–x**) and 0.4 (**y**, **z**, **aa**, **bb**), and wind speed (m s^{-1}), at 0.1 (**q**, **u**, **y**), 0.5 (**r**, **v**, **z**), 1 (**s**, **w**, **aa**) and 2 (**t**, **x**, **bb**), with leaf width (cm) of 0.04, 0.1, 0.5, 0.9, 1.5, 2.7 and 11 shown as increasing darker blue lines. No difference in leaf temperature from air temperature line in red. Two-tailed ordinary least square regressions were fitted for $\log(\text{trait}) = \log(a) + b \log(\text{climate variable})$ in **a–p**. *** $P < 0.001$, ** $P < 0.01$, * $P < 0.05$. $P = 2.1 \times 10^{-8}$ (**a**), 6.2×10^{-13} (**b**), 4.7×10^{-29} (**c**), 6.2×10^{-48} (**d**), 2.0×10^{-24} (**e**), 6.8×10^{-40} (**f**), 1.9×10^{-24} (**g**), 1.3×10^{-33} (**h**), 2.4×10^{-7} (**i**), 7.4×10^{-11} (**j**), 1.0×10^{-26} (**k**), 3.4×10^{-39} (**l**), 5.4×10^{-22} (**m**), 9.8×10^{-33} (**n**), 4.4×10^{-22} (**o**), 3.8×10^{-29} (**p**). C_3 and C_4 species are shown in red and blue, respectively.



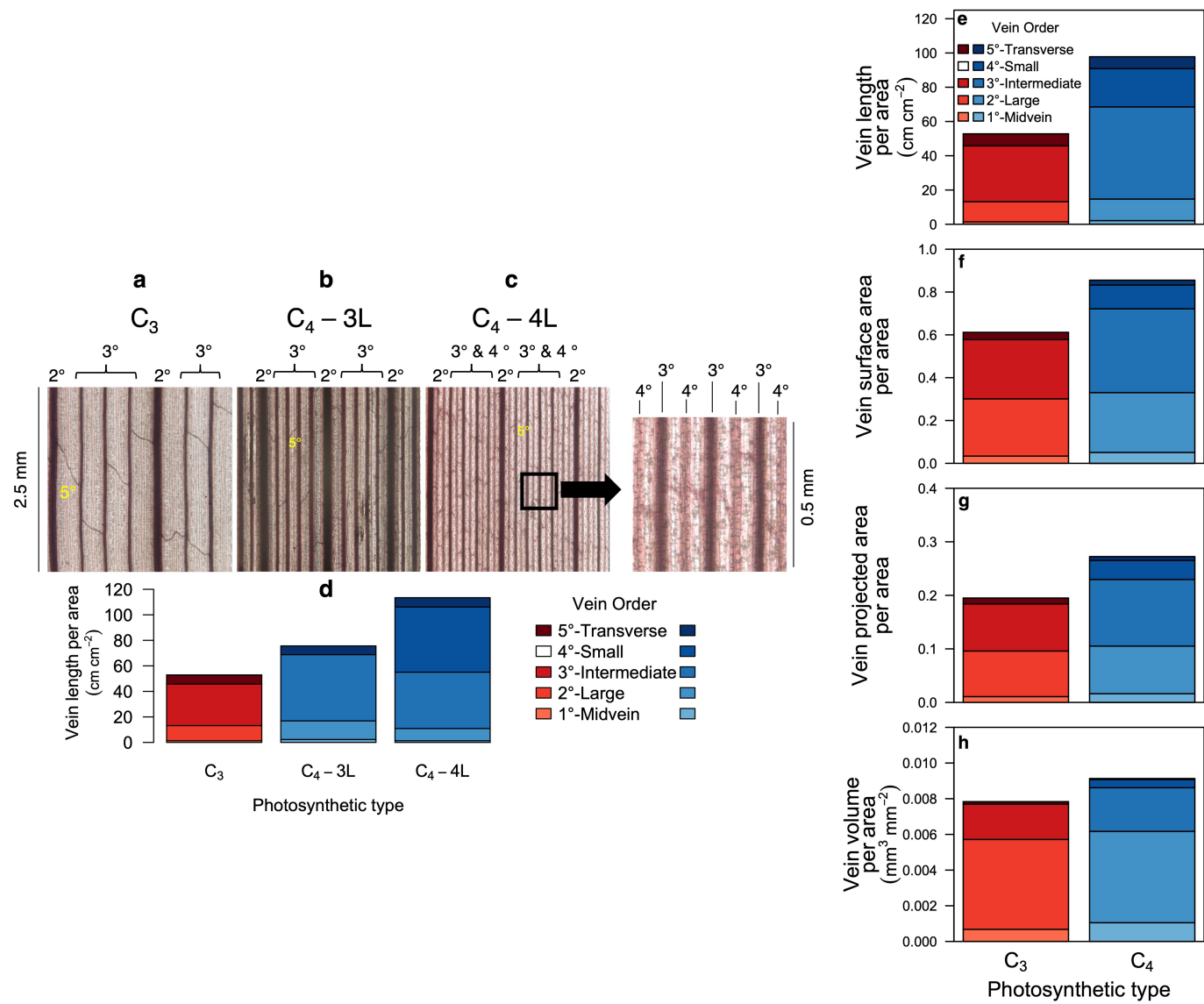
Extended Data Fig. 6 | Worldwide scaling of grass VLA and vein diameter with leaf size and aridity of the native climate of the species, and of vein xylem conduit diameter with vein diameter. **a-d**, Relationship of major VLA to leaf width (**a, c**), leaf area (**b, d**) and the aridity index (**e**) (in which lower values correspond to greater climatic aridity). **f-q**, Relationship of vein diameters to leaf length (**f, i, l, o**), leaf width (**g, j, m, p**) and leaf area (**h, k, n, q**). **r-z, aa, bb, cc**, Relationship of VLA to leaf length (**r, u, x, aa**), leaf width (**s, v, y, bb**) and leaf area (**t, w, z, cc**). **dd, ee, ff, gg**, Relationships of vein xylem conduit diameters with vein diameter of first-order veins (**dd**), second-order veins (**ee**), third-order veins (**ff**) and fourth-order veins (**gg**). $n = 616$ species in **a**, 600 in **b**, 170 in **c**, 166 in **d**, 21 in **e**, 27 in **f-z, aa, bb, cc, dd, ee, ff** and 7 in **gg**. Two-tailed ordinary least square regressions, PGLS or PRMA regressions were fitted for $\log(\text{trait}) = \log(a) + b \log(\text{trait or climate variable})$ in **a** and **b, c** and **d or e**, respectively. PRMA or

PGLS regressions were fitted for $\log(\text{vein diameter or VLA}) = \log(a) + b \log(\text{leaf length, width or leaf area})$ in **f-q** and **r-z, aa, bb, cc**, respectively. PRMA regressions were fitted for $\log(\text{xylem conduit diameter}) = \log(a) + b \log(\text{vein diameter})$ in **dd, ee, ff, gg**. * $P < 0.05$, ** $P < 0.01$, *** $P < 0.001$. $P = 9.4 \times 10^{-250}$ (**a**), 1.6×10^{-139} (**b**), 7.0×10^{-46} (**c**), 1.0×10^{-31} (**d**), 0.0051 (**e**), 0.0007 (**f**), 3.0×10^{-5} (**h**), 3.9×10^{-6} (**i**), 0.0003 (**k**), 1.2×10^{-34} (**s**), 7.0×10^{-4} (**t**), 1.4×10^{-7} (**v**), 0.0167 (**w**), 0.0020 (**bb**), 0.0110 (**dd**) and 0.0004 (**ee**). Line parameters for **f-z, aa, bb, cc** are given in Table 1, Supplementary Table 10; line parameters for **dd, ee, ff, gg** are given in Supplementary Table 11. Significant relationships are plotted with PRMA to illustrate the central trends (Methods). C_3 and C_4 species are shown in white and grey, respectively. The s.e. for species trait values are given in Supplementary Table 3.



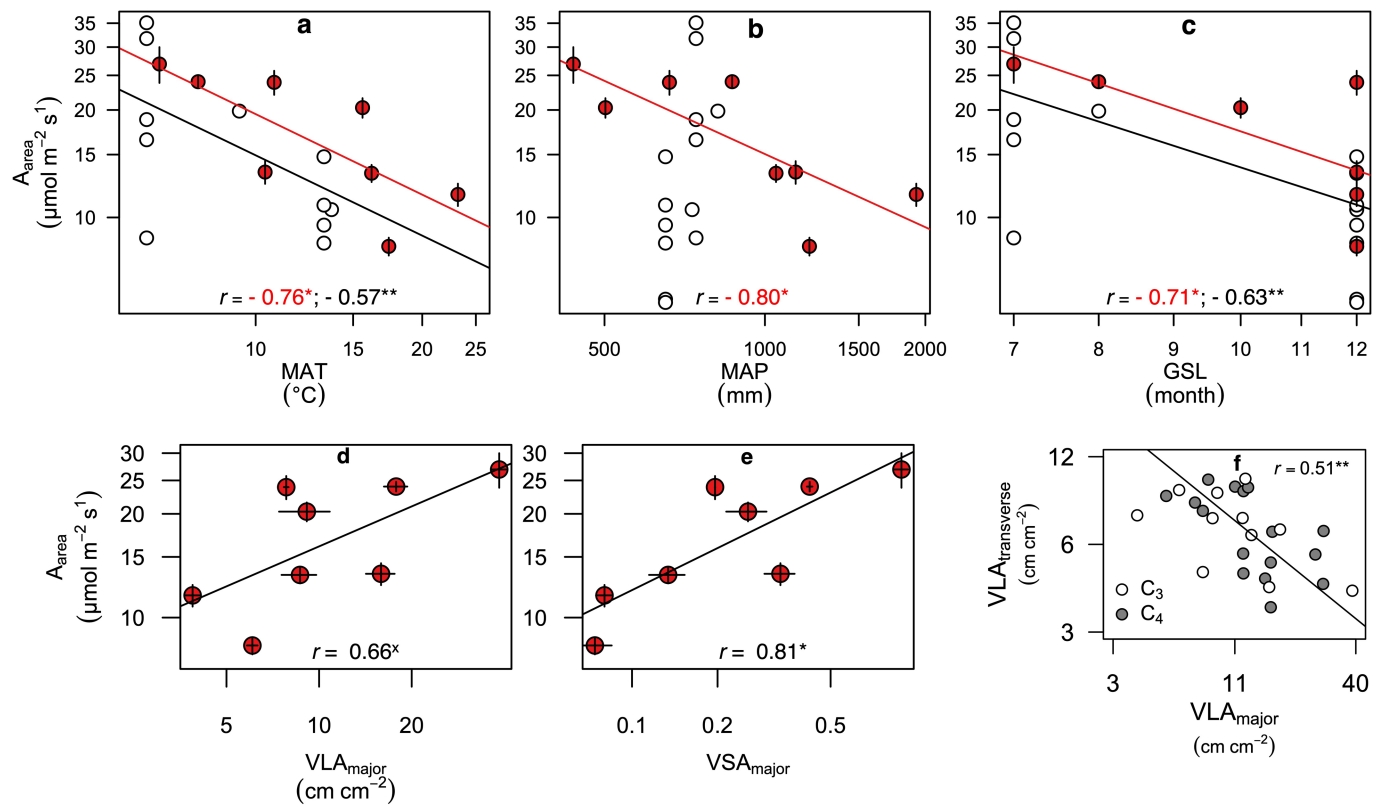
Extended Data Fig. 7 | Scaling of leaf vein projected area, vein surface area and vein volume of given vein orders with leaf dimensions across 27 grass species grown experimentally. **a–l**, Relationship of VPA to leaf length (**a, d, g, j**), leaf width (**b, e, h, k**) and leaf area (**c, f, i, l**). **m–x**, Relationship of VSA to leaf length (**m, p, s, v**), leaf width (**n, q, t, w**) and leaf area (**o, r, u, x**). **y, z, aa, bb, cc, dd, ee, ff, gg, ii**, Relationship of VVA to leaf length (**y, bb, ee, hh**), leaf width (**z, cc, ff, ii**) and leaf area (**aa, dd, gg, jj**). Two-tailed PGLS regressions were fitted for $\log(\text{VPA, VSA or VVA}) = \log(a) + b \log(\text{leaf length, width or area})$ and drawn

when significant. * $P < 0.05$, ** $P < 0.01$, *** $P < 0.001$; line parameters are given in Supplementary Table 10. $P = 0.0011$ (**a**), 1.2×10^{-12} (**b**), 0.0011 (**d**), 7.0×10^{-5} (**e**), 0.0335 (**g**), 0.0161 (**h**), 0.0167 (**k**), 0.0011 (**m**), 1.2×10^{-12} (**n**), 0.0011 (**p**), 7.0×10^{-5} (**q**), 0.0335 (**s**), 0.0161 (**t**), 0.0167 (**w**), 8.2×10^{-6} (**y**), 5.4×10^{-6} (**z**), 5.2×10^{-5} (**bb**), 0.0037 (**cc**), 0.0093 (**ff**). Significant trends are plotted with PRMA to illustrate the central trends (Methods). The s.e. for species trait values are given in Supplementary Table 3. C₃ and C₄ species are in white and grey, respectively.



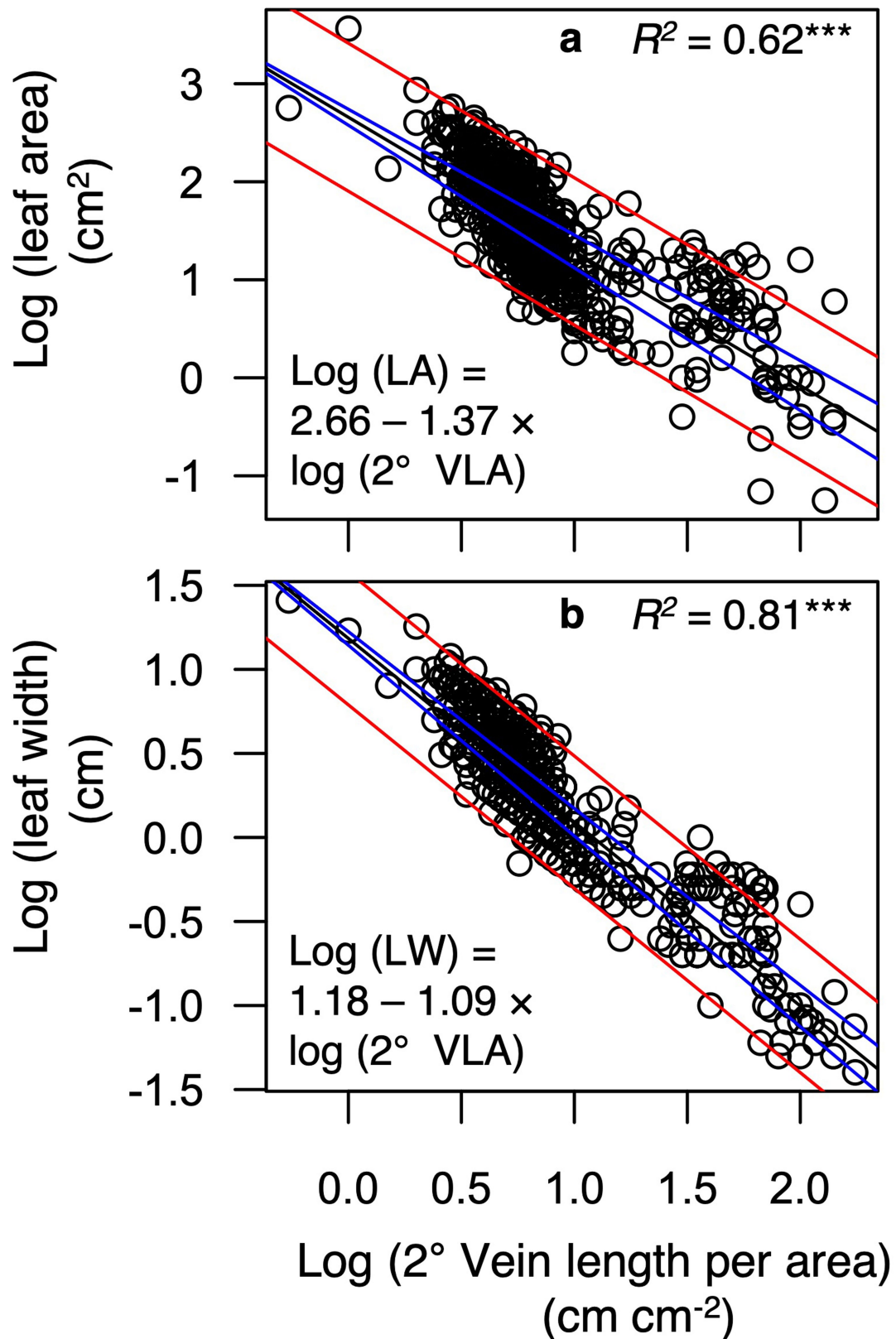
Extended Data Fig. 8 | Partitioning of the contributions of given vein orders of the venation architecture of C₃ and C₄ grasses, with minor veins accounting for the differences in VLA. **a**, *Triticum aestivum*, a C₃ species. **b**, *Aristida ternipes*, a C₄ species without fourth-order veins (C_{4-3L}) (that is, third-order veins are the highest longitudinal vein order). **c**, *Paspalum dilatatum*, a C₄ species with fourth-order veins (C_{4-4L}) (that is, fourth-order veins are the highest longitudinal vein order). **d**, VLA (cm per cm²) distribution across vein orders for each type (C₃, n = 11; C_{4-3L}, n = 9; C_{4-4L}, n = 7).

highest longitudinal vein order). **d**, VLA (cm per cm²) distribution across vein orders for each type (C₃, n = 11; C_{4-3L}, n = 9; C_{4-4L}, n = 7). **e–h**, VLA (e), VSA (f), VPA (g) and VVA (h) distribution across vein orders for each type (C₃, n = 11; C₄, n = 16). Statistical comparisons by phylogenetic ANOVA are given in Supplementary Table 3.



Extended Data Fig. 9 | Associations between light-saturated leaf photosynthetic rate and native climate and vein traits for terrestrial C₃ species, and the scaling of VLA of transverse fifth-order veins with major VLA in 27 C₃ and C₄ grass species grown experimentally. **a–c**, Relationship of area-based light-saturated photosynthetic rate (A_{area}) measured with photosynthesis systems and MAT (a), MAP (b) and growing season length (GSL) (c). **d–f**, Relationship of light-saturated photosynthetic rate per area and VLA_{major} (cm per cm²) (d) and major VSA (VSA_{major}, unitless) (e), and transverse VLA (VLA_{transverse}) (cm per cm²) with VLA_{major}. Points and lines in red represent eight terrestrial C₃ grasses (from this study) grown in a greenhouse common garden related to the mean climate of their native distribution, supporting the assumption of a higher photosynthetic rate in colder and drier climates with shorter growing seasons. Open points represent 13 Northern Hemisphere temperate terrestrial C₃ grass species from the global plant trait network (GLOPNET¹²⁶) measured in the field, as related to the mean climate at their field site. Black lines represent the significant trend through all the points in a, c, which—given the disparate data sources combined here (and the consideration of field site rather than native range climate for the GLOPNET species)—provides strong support for the generality of the relationships of

A_{area} to MAT and growing season length. Notably, these are conservative tests of the relationships of photosynthetic rate with native climate, as measurements of A_{area} that use the photosynthesis system chamber do not include the effect of the boundary layer conductance (which is made very high and invariant)²⁷. Under natural conditions (and especially under slow wind speeds), smaller leaves would have a boundary layer conductance higher than that of larger leaves (as shown in the simulation in Extended Data Fig. 5), and thus—under natural conditions that included the effects of boundary layer—a stronger trend would be expected for small-leaved species in colder and drier climates to have higher photosynthetic rates than larger-leaved species of warm, moist climates. Two-tailed ordinary least square regressions or PRMA were fitted for $\log(\text{trait}) = \log(a) + b \log(\text{trait or climate variable})$ in a–e and f, respectively. * $P < 0.05$, ** $P < 0.01$, ^x $P = 0.04$ in a one-tailed test of the hypothesized positive correlation. $P = 0.0301$ (red line in a), 0.0071 (black line in a), 0.0183 (b), 0.0474 (red line in c), 0.0021 (black line in c), 0.0794 (d), 0.0138 (e), 0.0061 (f). Error bars represent s.e. in a–e. The s.e. for species trait values in f are given in Supplementary Table 3. C₃ and C₄ species are shown in white and grey, respectively, in e.



Extended Data Fig. 10 | Estimating leaf size from venation traits that can be measured on small samples or fragments of grass leaves. **a, b,** Leaf area (**a**) and leaf width (**b**) predicted from VLA of second-order veins. $n=600$ and 616 species in **a** and **b**, respectively (Grassbase dataset, Supplementary Table 2). The relationships were fitted with two-tailed ordinary least square

regressions. These relationships enable the determination of intact leaf size from fragments that include at least two second-order veins (including fragmentary fossil remains). The 95% confidence intervals are in blue and 95% prediction intervals in red. *** $P < 0.001$. $P = 1.4 \times 10^{-127}$ (**a**), 7.6×10^{-227} (**b**).

Reporting Summary

Nature Research wishes to improve the reproducibility of the work that we publish. This form provides structure for consistency and transparency in reporting. For further information on Nature Research policies, see our [Editorial Policies](#) and the [Editorial Policy Checklist](#).

Statistics

For all statistical analyses, confirm that the following items are present in the figure legend, table legend, main text, or Methods section.

n/a Confirmed

- The exact sample size (n) for each experimental group/condition, given as a discrete number and unit of measurement
- A statement on whether measurements were taken from distinct samples or whether the same sample was measured repeatedly
- The statistical test(s) used AND whether they are one- or two-sided
Only common tests should be described solely by name; describe more complex techniques in the Methods section.
- A description of all covariates tested
- A description of any assumptions or corrections, such as tests of normality and adjustment for multiple comparisons
- A full description of the statistical parameters including central tendency (e.g. means) or other basic estimates (e.g. regression coefficient) AND variation (e.g. standard deviation) or associated estimates of uncertainty (e.g. confidence intervals)
- For null hypothesis testing, the test statistic (e.g. F , t , r) with confidence intervals, effect sizes, degrees of freedom and P value noted
Give P values as exact values whenever suitable.
- For Bayesian analysis, information on the choice of priors and Markov chain Monte Carlo settings
- For hierarchical and complex designs, identification of the appropriate level for tests and full reporting of outcomes
- Estimates of effect sizes (e.g. Cohen's d , Pearson's r), indicating how they were calculated

Our web collection on [statistics for biologists](#) contains articles on many of the points above.

Software and code

Policy information about [availability of computer code](#)

Data collection

Analyses were performed in the R programming language and environment (version 4.0.3). Trait data for the 1752 grass species from Kew Grassbase were provided by Dr. Maria Vorontsova personally. The corresponding 1752 species climate data were extracted from WorldClim 2.5-arc minute resolution (<https://worldclim.org/version2>) and from CRU TS4.01.01 (https://crudata.uea.ac.uk/cru/data/hrg/cru_ts_4.01/) based on each species' geographical records (<http://www.gbif.org>). We used the following packages to assist with data collection and data analyses: Taxonome (1.5), Taxonstand (2.2) and ape (5.4-1). Phylogenetic reconstruction was performed using the programs MUSCLE (<http://www.drive5.com/muscle/>), BEAST (<https://beast.community/>) and Tracer (<http://beadt.bio.ed.ac.uk/Tracer>). Comparative phylogenetic statistical analyses utilized the following R packages: phytools (0.7-70), nlme (3.1-151), phylogr (1.0.11), ape (5.4-1) and nortest (1.0-4). We utilized the R package tealeaves (1.0.5) to simulate grass leaf energy balance.

Data analysis

Data analyses were performed in the R programming language and environment (version 4.0.3) and code is available on Git-Hub (<https://github.com/smuel-taylor/grass-leaf-size->).

For manuscripts utilizing custom algorithms or software that are central to the research but not yet described in published literature, software must be made available to editors and reviewers. We strongly encourage code deposition in a community repository (e.g. GitHub). See the Nature Research [guidelines for submitting code & software](#) for further information.

Data

Policy information about [availability of data](#)

All manuscripts must include a [data availability statement](#). This statement should provide the following information, where applicable:

- Accession codes, unique identifiers, or web links for publicly available datasets
- A list of figures that have associated raw data
- A description of any restrictions on data availability

Data utilized in this study are provided in the supplementary materials. Leaf trait data for the 1752 grass species was provided by the published Kew Grassbase Database (<http://www.kew.org/data/grassbase/>). Species' climate data were extracted from WorldClim 2 5-arc minute resolution (<https://worldclim.org/version2>) and from CRU TS4.01 01 (https://crudata.uea.ac.uk/cru/data/hrg/cru_ts_4.01/) based on each species' geographical records (<http://www.gbif.org>). Photosynthetic trait data and field locations were extracted for the 13 C3 grass species for which this was available in GLOPNET (<http://bio.mq.edu.au/~iwright/glopian.htm>).

Field-specific reporting

Please select the one below that is the best fit for your research. If you are not sure, read the appropriate sections before making your selection.

Life sciences Behavioural & social sciences Ecological, evolutionary & environmental sciences

For a reference copy of the document with all sections, see nature.com/documents/nr-reporting-summary-flat.pdf

Ecological, evolutionary & environmental sciences study design

All studies must disclose on these points even when the disclosure is negative.

Study description

We tested for worldwide leaf size and climate relationships with the largest grass species set, using a phylogenetic comparative framework. We constructed an evolutionary conserved (across species) synthetic leaf development model that captures the temporal and spatial dynamics of leaf expansion with those of vein ontogeny, and provides predictions of how leaf vein traits would scale allometrically with leaf size dimensions. We explore the underlying adaptive physiological mechanisms that would underlie leaf size and climate relationships by 1) determining the role of the grass leaf boundary layer on leaf function and 2) testing predictions from the synthetic model that were confirmed across 27 diverse grass species grown in a common garden. Collectively, we show that small grass leaves have physiological advantages due to their smaller leaf boundary layer and by their vein traits that are constrained in smaller leaves. Such advantages, and the conservation of the leaf development model provide explanations for the distribution of grass leaf size globally.

Research sample

We extracted traits for 1752 grass species from the Kew Grassbase, the number of species for which both phylogenetic data and location information were available. This allowed us to test for global patterns of traits and climate while controlling for the influence of phylogenetic relatedness. We constructed the synthetic grass leaf development model from previously published studies on grass leaf development. Our common garden study utilized 27 grass species diverse in phylogenetic and ecological diversity, including 11 independent C4 origins, allowing us to test for diverse global scaling patterns of leaf vein traits and leaf size traits. In selecting these 27 species, we aimed to include as many independent C3 and C4 origin groups (i.e., distantly related sister taxa), and with diverse traits, to maximize the generality of our findings with respect to grass evolution and ecology. Thus, this smaller species set was designed to represent diverse grass species across the grass family.

Sampling strategy

Our sampling strategy was that of typical studies on comparative physiology, where measuring n = 3 individuals per species is sufficient to resolve statistical differences among species, especially when grown in a common garden. Standard errors for species' mean trait values are provided and their indication of significant species differences supports the sampling procedure.

Data collection

Alec extracted the 1752 leaf traits from the Kew Grassbase with assistance from Dr. Maria Vorontsova. Teera Watcharamongkol extracted the climate data for the 1752 species. Alec constructed the synthetic model and measured leaf traits for the 27 species in the common garden from previously sampled, processed, and imaged leaves.

Timing and spatial scale

Experimental data were collected from plants grown in a common garden November 2009 to June 2010, as described in the methods section, with leaf material fixed in formalin acetic acid, and measured for vein traits until January 2019.

Data exclusions

All experimental and field data are included in the supplements. We do not include data generated by our boundary layer simulations as we provide the specific simulation conditions that would replicate such data in the methods

Reproducibility

Plant growth was successful, and measurements were replicated on multiple individuals of each species as described in the Methods. We did not repeat the common garden experiment as this was not necessary to establish the trends shown, especially given their consistency with the trends shown in the global database.

Randomization

For our common garden study we spatially randomized individuals of different species within blocks, and replicated blocks throughout the growth center.

Blinding

Blinding was not relevant to our study, as experimenter bias would not influence our findings. The vein trait data, leaf size data and climate data were collected and analyzed separately, and compiled to test hypotheses after data collection was complete. Moreover, trends were also tested using published trait and climate data for the 1752 grass species from Grassbase, and for the 13 species from GLOPNET.

Did the study involve field work? Yes No

Reporting for specific materials, systems and methods

We require information from authors about some types of materials, experimental systems and methods used in many studies. Here, indicate whether each material, system or method listed is relevant to your study. If you are not sure if a list item applies to your research, read the appropriate section before selecting a response.

Materials & experimental systems

- | | |
|-------------------------------------|-------------------------------|
| n/a | Involved in the study |
| <input checked="" type="checkbox"/> | Antibodies |
| <input checked="" type="checkbox"/> | Eukaryotic cell lines |
| <input checked="" type="checkbox"/> | Palaeontology and archaeology |
| <input checked="" type="checkbox"/> | Animals and other organisms |
| <input checked="" type="checkbox"/> | Human research participants |
| <input checked="" type="checkbox"/> | Clinical data |
| <input checked="" type="checkbox"/> | Dual use research of concern |

Methods

- | | |
|-------------------------------------|------------------------|
| n/a | Involved in the study |
| <input checked="" type="checkbox"/> | ChIP-seq |
| <input checked="" type="checkbox"/> | Flow cytometry |
| <input checked="" type="checkbox"/> | MRI-based neuroimaging |